UNIVERSITY OF CALIFORNIA
RIVERSIDE

# Phase Manipulation of Fermionic Cold Atoms in Mixed Dimensions

A Dissertation submitted in partial satisfaction
of the requirements for the degree of

Doctor of Philosophy

in

Physics

by

Kyle Airell Irwin

December 2014

Dissertation Committee:

Professor Shan-Wen Tsai, Chairperson
Professor Roya Zandi
Professor Alexander Korotkov

The Dissertation of Kyle Airell Irwin is approved:

---

---

---

Committee Chairperson

University of California, Riverside

## Acknowledgments

First and foremost I'd like to thank my advisor, Shan-Wen Tsai. Without her guidance, patience, and encouragement none of this would have been possible. Shan-Wen has the rare gift of being able to balance deep scientific and mathematical understanding with an ability to communicate these concepts effectively to new students. After entertaining my nuanced technical questions she would always be willing to spend time in her office joking and discussing non-science related topics. I hope she recovers from Brazil's World Cup performance.

I'd like to thank my instructors for providing an enjoyable learning experience. Dr. Jose Wudka's lectures were a pleasure to attend; his ability to deliver the most technical details of a complex subject with logical clarity cannot be matched. I'd like to thank Dr. Vivek Aji for demystifying quantum many-body techniques both in the classroom and out. Vivek was always willing to sit with me, devoting his free time to my understanding of theoretical condensed matter techniques and ideas.

I'd also like to thank Dr. Chuntai Shi for our time spent discussing theoretical concepts and especially our lengthy discussions about the nuances of American and Chinese culture. Dr. Chen-Yen Lai, my group-mate was always available for rigorous discussion of renormalization group related material and I greatly appreciate that. Dr. Lingli Wang was the best office mate one could ask for, and I do believe we both enjoyed distracting each other from time to time with talk about anything other than science.

I made some amazing life-long friends during my stay at UCR. Dr. John Wyrick, his wife Satoko, and their dog Al are among my dearest friends. Those home-cooked dinners that turned into white-board discussions are some of my fondest memories. Thanks to my climbing buddies Ruben Ruiz and Morgan Mackie. Special thanks

to Juan, Liz, Tito, Tony, Shannon, Berto and the rest of the Apt. 32 crew for giving me a life outside of academia. Thanks to Joe Martinez for coffee, stimulating conversation, and nights at Pixels. Thanks to the Goodwin family and the entire staff at Goodwin's Organics for being the best neighborhood grocery store and coffee shop a guy could ask for. Last but not least I'd like to thank my girlfriend Desiré. You've always been there through the good and bad times. I don't think I could have made it this far without your love and support.

For Des

# ABSTRACT OF THE DISSERTATION

Phase Manipulation of Fermionic Cold Atoms in Mixed Dimensions

by

Kyle Airell Irwin

Doctor of Philosophy, Graduate Program in Physics
University of California, Riverside, December 2014
Professor Shan-Wen Tsai, Chairperson

Ultra-cold fermionic atoms trapped in optical lattices may be a candidate for the discovery of novel phenomena in condensed matter systems. Experiments afford the creation of virtually any lattice geometry, and physical parameters of tight binding type lattice models can be acurately and easily tuned. Although some theoretical work has been conducted, few have used the power of the functional renormalization group method to unearth rigorous methods for determining collective many-body phases in this regime. Motivated by recent experimental achievements, we investigate novel condensed matter systems involving interacting fermions which are engineered to be confined in different dimensions. In this sense, we seek low energy effective theories for low-dimensional fermionic lattice systems embedded into higher dimensional lattice systems, and show how tuning physical quantities, such as the filling or density, can have dramatic effects on the behavior of the lower dimensional system.

# Contents

# List of Figures

# Chapter 1

# Introduction

The present work focuses on the classification of the phases that emerge in a relatively new branch of theoretical and experimental condensed matter physics: systems with mixed species of fermions made to come together and interact in different dimensions. We'll examine a system of one-dimensional fermions embedded into a square lattice of a different species. The particulars of one-dimensional conducting systems and renormalization group results on them have been an area of intense study in years past. The work to follow should seem familiar to veterans of the field, but should also pique their curiosity with regard to the expansion into density-controlled phase manipulation. The idea of the one-dimensional line embedded into a square lattice may be extended to ladder systems which involve two one-dimensional lines interacting with each other in addition to their interactions with the surrounding two-dimensional lattice. The work was inspired by experimental developments in the field of ultra-cold atoms trapped in atomic lattices.

Cold atom systems have proven to be an invaluable tool in studying a wide range of condensed matter phenomena. Relative ease in experimental tuning of inter-

particle interactions and the ability to create various lattice geometries are notable examples of the field's breadth. Of particular interest is the creation of systems with mixed species and dimensionality; these experimentally realizable systems are central to the research presentation to follow.

In the early days of using cold atom systems to model condensed matter systems, much of the focus dealt with the realm of bosonic theories; in particular, much interest was generated in expanding the knowledge of Bose-Einstein condensates (BECs). Initially efforts were made to explain condensate properties of matter waves of weakly interacting quantum gases [17, 38, 54, 53], and later evolved to include the effects of strong coupling regimes [28]. These systems can be made to trap cold atoms in one, two, or three dimensional lattice configurations by (effectively) creating uniform, steady-state electric fields with overlapping laser light. The atoms are constrained to exist *only* at these lattice sites, and may only "move" onto other lattice sites. In essence, cold atoms trapped in optical lattices can be efficiently made to mock tight-binding and Hubbard-like models [26, 5].

More recent experiments have shifted focus to Fermionic atoms [74, 51, 73, 60], and a multitude of exotic phenomena normally not occuring in condensed matter systems can now be fabricated with exceptional tunability via controllable parameters [29, 7, 55, 62, 70, 12, 43, 44, 22]. For instance, fermionic mixtures can be manipulated to carry different internal properties such as population densities, group symmetries, lattice geometries, and dimensionalities. By cooling two fermionic isotopes of ytterbium with different nuclear spins, a degenerate fermi mixture with an $SU(2) \times SU(6)$ symmetry has recently been achieved [63]. Mixed two-species fermi gases with unequal populations have also been extensively studied [52, 61], as well as systems of dipolar atoms and molecules [41, 30, 23]. Many-body effects in these systems can be further

enhanced when the system is loaded onto an optical lattice [8] and interactions tuned via Feshbach resonances [16, 64, 66]. Fermions with imbalanced populations [36] and dipolar fermions [21, 20] on a square lattice have been investigated and present a much richer phase diagram than their gas counterparts, with lattice effects enhancing the transition temperature for various phases.

Experimentally, it is also possible to confine components of an ultra-cold atom mixture in different dimensions [37], and this has triggered some recent theoretical studies [48, 50, 27]. As pointed out by Nishida [47],the mediated intra-species interaction generated may in fact reshape the phase diagram in a bi-layer fermi gas. Furthermore, Efimov physics with fermions is also proposed to energy in one/three-dimensional mixed systems [49]. The properties of the lower-dimensional fermi gas can be manipulated by tuning parameters in the higher dimensional species; it is precisely these inter-dimensional interacting systems which form the bulk of the current research, and will be discussed in the chapters to follow.

It was, in fact, the mixed-dimensional variety of cold atom systems which provided the impetus for the current research. In particular the work of Lamporesi et al. [37], in which $^{41}K$ atoms were made to "live" on a two-dimensional lattice while $^{87}Rb$ atoms are confined to a three-dimensional lattice, provided much of the inspiration. In light of this experimental success, some theoretical work was conducted [48, 27] wherein quantum phases were investigated.

Chapter 2 provides the historical context of the renormalization group method for understanding why phase transitions occur in principle. Kadanoff's scaling hypothesis is discussed, and Wilson's renormalization group formulation is shown to be a rigorous derivation of the scaling hypothesis. From this historical motivation, the renormalization group technique is developed for one-dimensional fermionic systems at half-filling.

The analysis results in a set of "flow equations" which govern the behavior of particular couplings which in turn determine the phase of the system.

Chapter 3 introduces the mixed 1D/2D system engineered out of ultra-cold atoms trapped in optical lattices and applies the renormalization group technique to determine the phases of the system. The effect of the two-dimensional system manifests itself in the form of a mediated interaction. This effective interaction between one-dimensional particles plays a crucial role in the collective phase of the one-dimensional system. A detailed analysis of the behavior of the four unique couplings, known collectively as the "g-ology", is conducted in a space parameterized by the mediated interaction at momentum transfers of 0 and $\pi$ between particles of the same spin.

Chapter 4 extends the idea of chapter 3 one dimension further by considering a two-leg ladder embedded into a square lattice. The phase diagram of the system is discussed and shows how phase manipulation exists (as with the 1D/2D system) by tuning the density of the larger dimensional system.

# Chapter 2

# Renormalization Group For One-Dimensional Interacting Fermions at Half-Filling

## 2.1 Motivation

In essence this work is an exposition on the Renormalization Group technique applied to one-dimensional and, in the case of the two-leg ladder, quasi-one-dimensional conducting systems. There exist many excellent reviews on the subject matter [58, 72, 9] and this chapter merely serves to summarize the relevant issues insofar as to make the treatise on the mixed-dimensional systems to follow self-contained.

Historically, the renormalization group was used by Wilson [71] to show that the Widom-Kadanoff scaling laws [31] used to explain how various physical couplings should be (length-) scale dependent, could be derived through rigorous mathematical means on a microscopic level. This analysis was famously used to discuss continuous

phase transitions of the Ising model for ferromagnetism. The partition function for the system is given by

$$\mathcal{Z}(K,h) = \sum_{\{S\}} e^{K\sum_{\vec{R}}\sum_{\vec{i}} S_{\vec{R}}S_{\vec{R}+\vec{i}}+h\sum_{\vec{R}} S_{\vec{R}}} = e^{-\beta F} \tag{2.1}$$

and describe a lattice of spins coupled to a local magnetic field $h$ with interactions between nearest neighboring spins with strength $K = -\beta J$. Kadanoff proposed that as the temperature of the system approaches a critical value ($K \to K_c$) the free energy $F$ develops a singularity. Furthermore, an "order parameter" is defined for the system whose features change drastically as the temperature is lowered below the critical temperature. In the Ising model this order parameter is the expectation value of the magnetization $\langle M\rangle = 1/N \sum_{\vec{R}}\langle S_{\vec{R}}\rangle$

Kadanoff (erroneously) imagined a scheme where instead of summing over each configuration of spins, the spins were "unified" over cubic blocks of size $L^d$, in effect replacing the theory of single spins with an equivalent theory in terms of appropriately normalized "block spins." He then hypothesized that the functional form of the free energy $F$ was precisely the same: having blocked the spins one can define new couplings, local magnetic field strength, and order parameter such that $K \to K_L$, $h \to h_L$, and $\langle M\rangle \to \langle \mu\rangle$. Kadanoff then proposed that the transformation from spins to block spins leaves the free energy *invariant*. This consistency requires the free energy and correlation length to satisfy the scaling laws

$$F(K,h) = L^{-d}F(k_L,h_L) \tag{2.2}$$

$$\xi(K,h) = L\xi(K_L,h_L) \tag{2.3}$$

After $n$ blocking transformations, the correlation length in 2.3 may be inverted

to give $\xi(K_{L^n}, h_{L^n}) = \xi(K_0, h_0)/L^n$ where $K_0$ and $h_0$ are the initial values in the unblocked system. As the blocking procedure carries on, the couplings find their way to fixed values referred to as "fixed points" [67] which will be denoted as $K^*$ and $h^*$. Once these fixed points have been reached, the correlation length satisfies

$$\xi(K^*, h^*) = \frac{1}{l}\xi(K^*, h^*) \tag{2.4}$$

which implies that the correlation length must be either zero or infinity. Critical correlations that grow to infinity form the basis of a microscopic understanding of phase transitions.

While there is no reason to believe that the free energy should remain the same after each blocking transformation in the Ising model, Kadanoff's approach contains the essence of the modern renormalization procedure:

- Classification of a phase transition requires the identification of an *order parameter*. As the system reaches criticality the order parameter acquires a non-zero value of which there may be many.

- Fluctuations of an order parameter grow as the system reaches criticality and the correlation length of these fluctuations becomes infinite as signaled by a diverging susceptibility.

- Long-wavelength physics (long-range fluctuations) of the system are found by integrating out high-energy terms in the partition function of the system, utilizing the renormalization group technique. On each differential iteration of the process, the action of the system is invariant.

- The flow of the couplings in the action is, as Wilson suggested, determined by a

differential equation referred to as the "beta function."

## 2.2 Renormalization Group for Interacting Hubbard Fermions at Half-Filling

With the tenets of the renormalization group procedure outlined in the previous section, one begins the analysis by constructing the many-body coherent state path integral for interacting fermions.

$$\mathcal{Z} = e^{-\beta\Omega} = \text{Tr } e^{-\beta(\hat{H}-\mu\hat{N})} = \int \mathcal{D}\big[\bar{\phi}\phi\big]\, e^{-S(x,\tau)} \tag{2.5}$$

where the action, $S(x,\tau)$ is given by

$$S(x,\tau) = \sum_i \int_0^\beta d\tau \left[\bar{\phi}_i(\tau)\partial_\tau\phi_i(\tau) + \hat{H}(\bar{\phi}_i(\tau)\bar{\phi}_i(\tau)) - \mu\hat{N}(\bar{\phi}_i(\tau)\bar{\phi}_i(\tau))\right] \tag{2.6}$$

and $\bar{\phi}_i(\tau)$ ($\phi_i(\tau)$) is shorthand for the creation(annihilation) operators replaced by Grassman fields by taking the trace with respect to fermionic coherent states, and the index $i$ refers to the single-particle basis the second-quantized Hamiltonian was constructed with (in this case the momentum basis). The Hamiltonian is composed of two terms $\hat{H} = \hat{H}_0 + \hat{H}_I$. After performing a Fourier transform from $\tau \to \omega_n = (2n+1)\pi/\beta$, the Matsubara frequencies, the total action decomposes into two terms given by

$$S_0 = \sum_{k,\omega,\sigma} \bar{\phi}_\sigma(k\omega)\left[-i\omega + \epsilon(k) - \mu\right]\phi_\sigma(k\omega) \tag{2.7a}$$

$$S_I = \frac{1}{2}\sum_{\{k\omega\}} U(\{k\omega\})\bar{\phi}_\sigma(4)\bar{\phi}_{\sigma'}(3)\phi_{\sigma'}(2)\phi_\sigma(1)\bar{\delta}(k_1+k_2-k_3-k_4)\delta(\omega_1+\omega_2-\omega_3-\omega_4) \tag{2.7b}$$

The numbers appearing in the Grassman fields are a shorthand notation $\phi(i) \equiv \phi(k_i\omega_i)$ and $\{k\omega\}$ indicates the set of momenta and Matsubara frequencies with labels 1 through 4. The bar over the momentum conserving delta function indicates that the momenta

$k_1 \ldots k_4$ are conserved up to a reciprocal lattice vector, and in the case of fermions on a one-dimensional lattice the reciprocal lattice vectors correspond to $2n\pi$ for $n = \pm 1, \pm 2, \pm 3, \ldots$ where the lattice constant has been set to unity.

In keeping with the mantra laid out in the previous section, the aim is to discover the long-range physics of the system. To this end, a *mode elimination* is performed in which the short-wavelength terms (high energy terms) in the action are explicitly integrated out. The high energy terms are those residing the furthest away from the "fermi surface" - a manifold of $k$-values that satisfy $\epsilon(k) - \mu = 0$. In one dimension, this surface consists of exactly two points, and at half filling (half as many fermions as there are lattice sites) these two points lay at $\pm\pi/2$. If the system is very cold, then it stands to reason that all of the dynamics take place within a tight proximal region around the fermi points. Taking this into account, a *cutoff* is introduced within which all the dynamics of the system take place. Alternatively, one could imagine having partially integrated the partition function from the edges of the full bandwidth, renormalizing the action at each differential step, but being far enough away from the long-range features of the system to have avoided any divergences.

The action has now been reduced to terms residing within a narrow band centered around the two fermi points. For one-dimensional fermions on a lattice restricted to nearest-neighbor hopping, the dispersion may be replaced with its linearized form

$$\begin{aligned} \epsilon(k) &= -2t\cos(k) \\ &\simeq \pm 2t(k \pm \pi/2) = \pm v_F(k \mp \pi/2) \end{aligned} \tag{2.8}$$

where $v_F$ is the *fermi velocity* and the upper (lower) sign refers to the linearized dispersion near the right (left) fermi point. By taking the thermodynamic limit ($N \to \infty$) and letting the temperature go to absolute zero, the sums in the action are replaced with

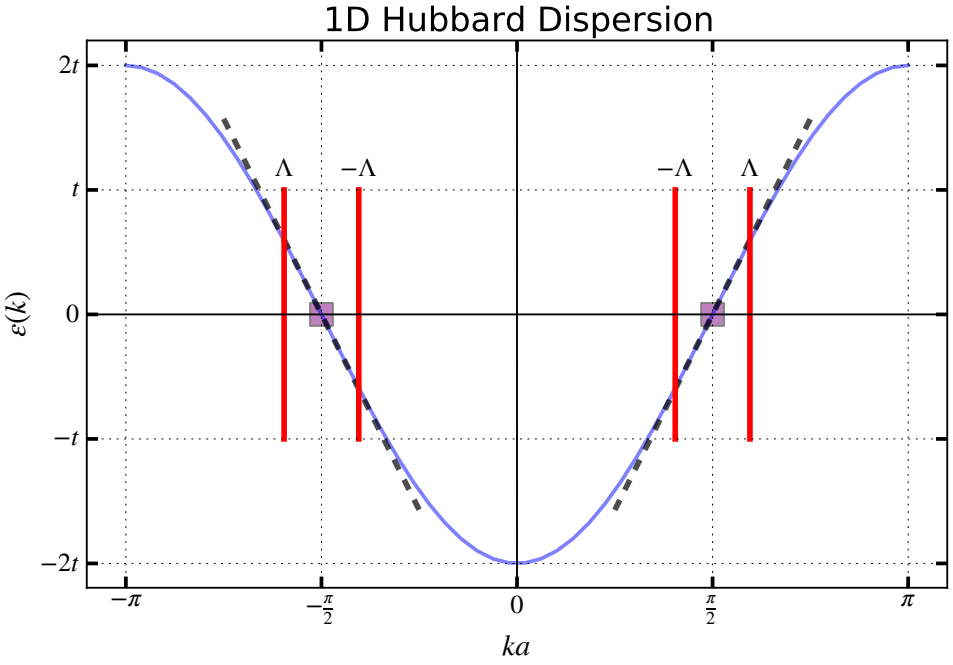


Figure 2.1: Dispersion for fermions on a one-dimensional lattice. The black dotted line denotes the linearized form of the energy applicable within the narrow cutoff (red lines at $\pm\Lambda$) of the left and right fermi points (purple squares).

the integrals

$$\frac{1}{N}\sum_{k} \to \int \frac{dk}{2\pi} \tag{2.9a}$$

$$\frac{1}{\beta}\sum_{\omega} \to \int \frac{d\omega}{2\pi} \tag{2.9b}$$

To begin the mode elimination the fields in the action must be divided into those which are *slow* and those which are *fast*. This is done with respect to a shell of energy around the fermi points of value $\Lambda$ as indicated by the red bars in fig.2.2. As such, the fields divide as

$$\phi_\sigma(k\omega) = \Theta(|\xi(k\omega)| - \Lambda)\phi_{>\sigma}(k\omega) + \Theta(\Lambda - |\xi(k\omega)|)\phi_{<\sigma}(k\omega) \tag{2.10}$$

The slow modes are inside the shell $\pm\Lambda$ while the fast ones are outside. The cutoff is only defined with respect to momentum space, while the Matsubara frequencies are left unaltered. In this sense, the action now takes the form

$$\begin{aligned}
\mathcal{Z} &= \int \mathcal{D}_< e^{S_0(\bar{\phi}_<\phi_<)} \int \mathcal{D}_> e^{S_0(\bar{\phi}_>\phi_>)} e^{S_I(\bar{\phi}_<\phi_<\bar{\phi}_>\phi_>)} \\
&= \mathcal{Z}_> \int \mathcal{D}_< \langle e^{S_I(\bar{\phi}_<\phi_<\bar{\phi}_>\phi_>)} \rangle_> \\
&= \int \mathcal{D}_< e^{\left(S_0(\bar{\phi}_<\phi_<) + S_I(\bar{\phi}_<\phi_<) + \ln\langle e^{S_I(\bar{\phi}_<\phi_<\bar{\phi}_>\phi_>)}\rangle_> + \ln\mathcal{Z}_>\right)}
\end{aligned} \tag{2.11}$$

This low energy effective action (LEEA) now represents the system at a lower energy, closer to the fermi energy, and consequently contains the physics at longer wavelengths.

$S_0(\bar{\phi}_<\phi_<)$ represents the kinetic part of the action which contains *only* the slow modes. As a true renormalization, it retains the exact same funcitonal form as the action before and mode elimination took place. $S_0(\bar{\phi}_>\phi_>)$ is the kinetic part of the action but contains purely fast modes. $S_I(\bar{\phi}_<\phi_<\bar{\phi}_>\phi_>)$ represents the interacting

part of the action containing both slow and fast modes. The notation $\langle A \rangle_>$ represents the statistical average of the quantity $A$ taken with respect to only the fast modes. $\ln \mathcal{Z} = \beta \Omega_>$ is the grand canonical potential [14] of the fast modes written for an action consisting of purely fast modes; this term merely shifts the free energy and can be disregarded.

Evaluating the natural log of the fast average involves invoking the so-called linked cluster theorem [46] in which only "connected" Feynman diagrams contribute. This is an expansion of connected contractions of $S_I^n$ for $n = 1, 2, 3, \ldots$ that generates terms in the LEEA containing two, four, six, etc. slow fields once the fast modes have been integrated out. These terms are responsible for changes in the action. Terms with odd mixes of slow and fast modes are possible since they can be contracted with similar terms, but these don't represent changes to terms present before mode elimination happened.

Collecting all the terms in the new LEEA we see that both the kinetic and interacting terms are modified, and terms consisting of higher numbers of slow fields are generated (although once the scaling of the action is discussed these terms will be dubbed "irrelevant," and renormalize to zero eventually). Terms with two remaining slow fields in the linked cluster expansion modify the kinetic terms on each renormalization step. In principle these are collected and grouped with the chemical potential. Terms containing four slow fields renormalize the interaction. Each renormalization step will produce the terms that existed at the previous energy scale. These terms are referred to as "tree level" terms.

In the present work, only contractions at "one loop" are considered since they are essentially the lowest order terms in an expansion of powers of the (weak) interaction

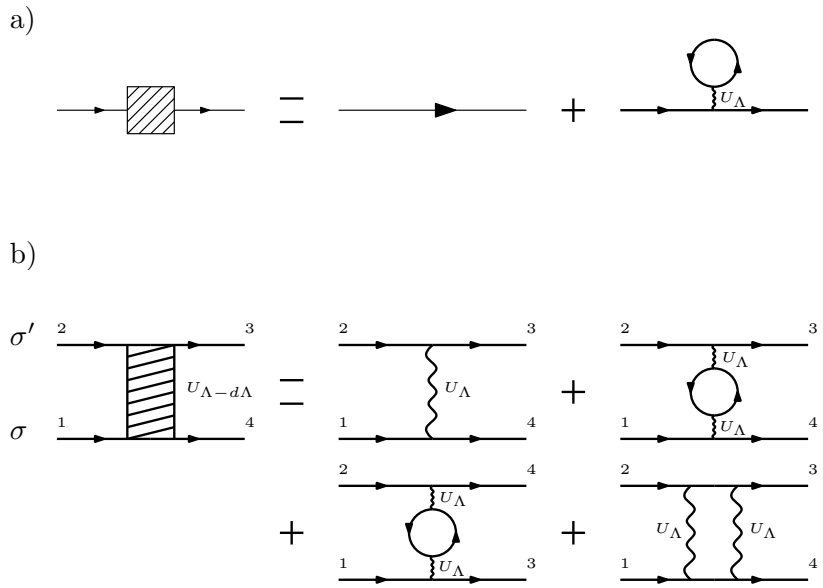


Figure 2.2: Feynman diagram schematic for the fast-field contracted terms that renormalize the action to one loop. *a*)The renormalized kinetic term is a sum of the tree level kinetic energy and $\langle S_I \rangle$ with two contracted fast modes. *b*)Corrections to the interaction consist of the tree level interaction plus the ZS, ZS', and BCS terms as shown in succession.

$U$. A schematic of the renormalized terms in the action are shown in Fig.2.2

## 2.3 Scaling of the Renormalized Action

In the previous section the diagrammatic expansion of the renormalization was considered. By performing a mode elimination, breaking the action of the partition function into slow and fast modes (long and short wavelength physics) , and partially integrating out the fast modes, a low energy effective action was found for an energy scale closer to the fermi points. The new action, however, is written for a subset of the original bandwidth of momenta. By performing a rescaling of the terms, the new low energy effective action retains the *exact* form but with physical quantities rescaled.

Firstly, one must replace the momenta and dispersion with those written with respect to the fermi points. In this sense the dispersion in Eq. 2.8 becomes $\epsilon_i(K)v_F K$

with $K = |k| - k_F$ and the subscript $i$ refers to the right or left fermi points. The integral over the momentum is limited by the cutoff as

$$\int_{-\Lambda}^{\Lambda} \frac{dK}{2\pi} \tag{2.12}$$

By introducing the scaling parameter $s$, the momenta remaining after a mode elimination lay in the range $-\Lambda/s \leq |K| \leq \Lambda/s$ while the fast modes that have been eliminated in the previous renormalization step lay in the range $\Lambda/s \leq |K| \leq \Lambda$. To make the new LEEA a fixed point of the interaction, one defines new scaled momenta, Matsubara frequencies, and fields according to

$$K' = sK \tag{2.13a}$$

$$\omega' = s\omega \tag{2.13b}$$

$$\phi(K'\omega') = s^{-3/2}\phi(k\omega) \tag{2.13c}$$

Terms that renormalize the kinetic energy are diagonal in $k, \omega, \sigma$. Schematically they are represented by the second diagram in Fig. 2.2a and have the explicit form

$$\delta S_2 = \sum_{i\sigma}^{L,R} \int_{\Lambda/s}^{\Lambda/s} \frac{dK}{2\pi} \int \frac{d\omega}{2\pi} \Gamma_2(K\omega)\bar{\phi}_{i\sigma}(K\omega)\bar{\phi}_{i\sigma}(K\omega) \tag{2.14}$$

By implementing the scaling of Eq.(2.13) the one-body function $\Gamma(K\omega)$ scales as

$$\Gamma(K'\omega') = s\Gamma(K\omega) \tag{2.15}$$

By expanding the one-body function in a Taylor series expansion in both $K$ and $\omega$, the relevance of each term may be examined under the scaling procedure. This expansion goes as

$$\Gamma(K\omega) = \Gamma_{00} + \Gamma_{10}K + \Gamma_{01}i\omega + \cdots + \Gamma_{mn}K^m(i\omega)^n \tag{2.16}$$

and indicates that $\Gamma_{00} \to s\Gamma_{00}$, i.e. that it is a *relevant* parameter. As $s \to \infty$ reducing the cutoff closer to the fermi surface upon each renormalization step, $\Gamma_{00}$ diverges. The next two terms have no dependence on $s$ after all substitutions of Eq.(2.13) are made and this type of parameter is said to be *marginal*. The remaining terms in the series scale as some negative power of $s$ and as such renormalize to zero.

A similar method applies to the terms with four fields that renormalize the interaction. These are the tree level, ZS, ZS', and BCS terms in the diagrammatic expansion in Fig. 2.2b. Each has four "external" legs of the diagram corresponding to the four slow modes that were untouched during the mode elimination. The external legs lay in the region of the Brillouin zone bounded by $\pm\Lambda/s$.

First consider the tree level term which contains purely slow modes and comes about when all the integrals over momentum are limited by $-\Lambda/s \leq |K| \leq \Lambda/s$ After scaling the momenta, Matsubara frequencies, and fields, and Taylor expanding the renormalized interaction around the fermi points we discover that the constant term is marginal and the rest are irrelevant. In one dimension it is, in fact, the flow of couplings evaluated *precisely* at the fermi points in all possible combinations that are allowed for by the momentum conserving delta function. In total there are only four distinct scattering processes in this sense and are shown in Fig. 2.3.

The next 3 terms in Fig. 2.2b contain an integral over momenta in the range $\Lambda/s \leq |K| \leq \Lambda$. These terms are proportional to two coupling functions each containing two slow and two fast modes. The fast modes between the two coupling functions are contracted leading to two Green's functions. The topology of the different diagrams

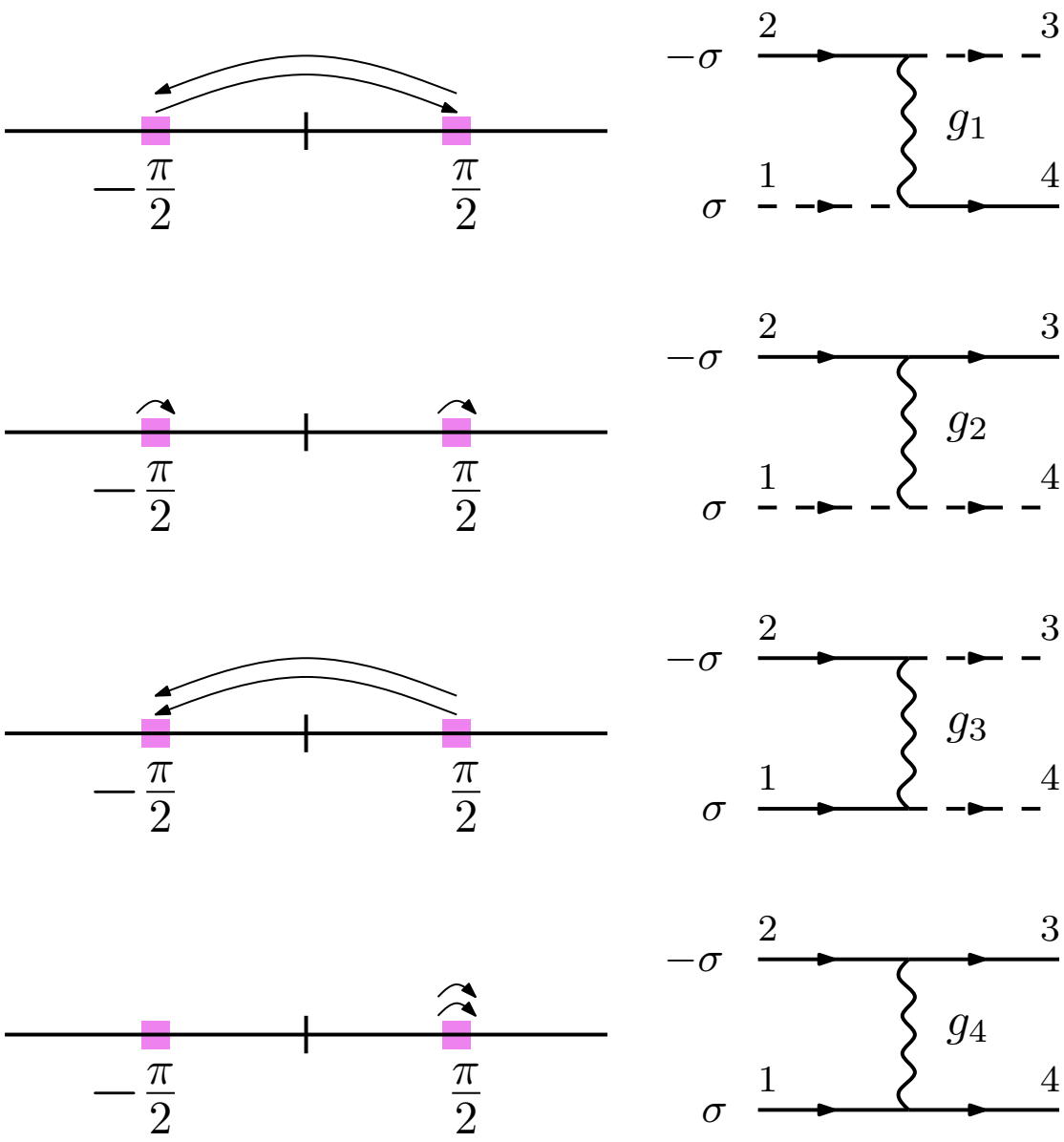


Figure 2.3: Four unique one-dimensional scattering processes for chemical potential $\mu = 0$ (which allows for Umklapp scattering) referred to as the "g-ology":$g_1$ is back scattering, $g_2$ is the forward scattering, $g_3$ is the Umklapp scattering, and $g_4$ is an additional type of forward scattering.

indicates which of the momenta 1 through 4 in each coupling function is taken as fast and slow, and it's symmetries will determine if it can contribute to the one-loop correction of the different terms making up the g-ology. Ultimately these terms are proportional to two factors of a marginal coupling (the topology of the particular diagram determining which of the four unique scatterings from the g-ology), and to a factor of $\Delta\Lambda/\Lambda$. $\Delta\Lambda$ is the size of the shell of fast modes eliminated during the renormalization step. Thus at tree level, the different couplings are still marginal and it is left to the one-loop term to determine how the coupling flows under the RG process.

## 2.4 Differential Renormalization and the Flow Equations

In the last section scaling was applied to the renormalization procedure to determine how the various terms in the action would change as the renormalization procedure cranked on. Scaling provided the machinery to determine which terms to keep track of during renormalization but in what follows the process of reducing the Brillouin zone to the fermi points will be handled in a more controllable manner.

The originally placed cutoff defining the effective limit of low energy physics will be dubbed $\Lambda_0$. The process of eliminating fast modes will be conducted by defining a floating energy surface parameterized by a renormalization step $l$ by defining

$$\Lambda(l) = \Lambda_0 e^{-l} \tag{2.17}$$

and taking the action through a series of infinitesimal model eliminations defined by

$$S_{\Lambda_0} \to S^1_{\Lambda_0 e^{-dl}} \to S^2_{\Lambda_0 e^{-2dl}} \to \dots \tag{2.18}$$

At each step $\Lambda dl$ of modes are eliminated at a distance of $\Lambda(l)$ from either side of

the two fermi points. In what follows it is imagined that the renormalization process has been cranking on, starting from the original cutoff $\Lambda_0$ and proceeding down to $\Lambda(l) = 0$ at which point it will be exactly at the fermi points. In this sense the diagrammatic combination of four-field terms in Fig. 2.2b becomes a differential equation governing the flow of the coupling functions (the g-ology) from their initial values at $l = 0$. Under this scheme the flow equations for the four unique one-dimensional scatterings are functions of the renormaliation step $l$ and satisfy

$$\frac{dg_1}{dl} = -g_1^2 \tag{2.19a}$$

$$\frac{d}{dl}(2g_2 - g_1) = g_3^2 \tag{2.19b}$$

$$\frac{dg_3}{dl} = g_3(2g_2 - g_1) \tag{2.19c}$$

$$\frac{dg_4}{dl} = 0 \tag{2.19d}$$

Before closing this section it is important to discuss the correlation functions. As previously stated, a phase transition should be accompanied by a diverging correlation length. Strictly speaking, the correlation function associated with a particular order parameter changes as the renormalization procedure cranks on. As such a differential equation for the correlation function must be obtained in the same vein as the flow equations for the g-ology. Similar to the Ising model in Eq.(2.1) the correlation function's flow equation can be calculated by adding a set of source fields to the action which couple to the order parameter as

$$S(\bar{\phi}, \phi, h_\delta) = S(\bar{\phi}, \phi) + \sum_{\delta q} (h_\delta^*(q)\Delta_\delta(q) + \text{h.c.}) \tag{2.20}$$

With this addition, the correlation function may be calculated as a derivative of the thermodynamic potential as

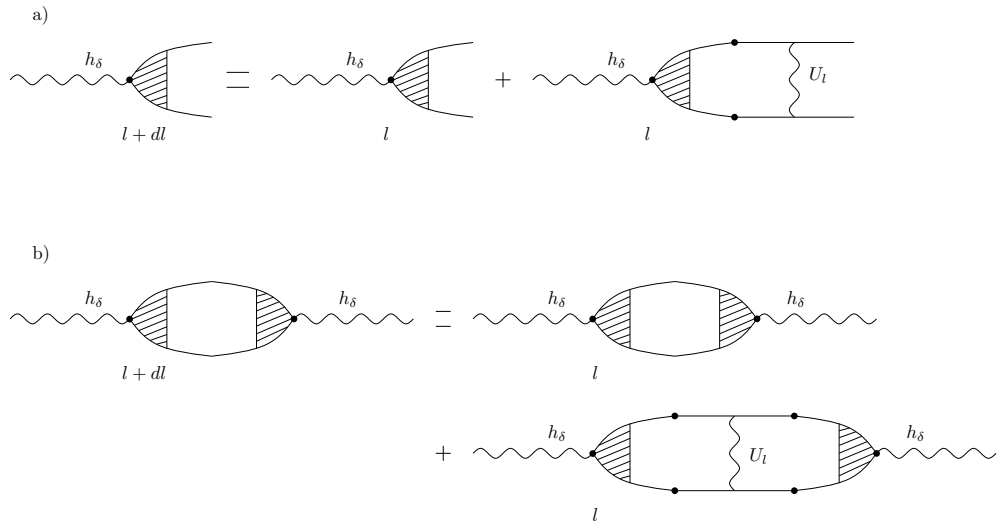


Figure 2.4: Diagrammatic representation of the renormalization process for the *a*) 2-point vertex $z_\delta(l, q)$ and *b*) correlation function.

$$\chi = -\beta \frac{\partial \Omega}{\partial h^*_\delta(q) \partial h_\delta(q')} = -\langle \bar{\Delta}_\delta(q) \Delta_\delta(q') \rangle \tag{2.21}$$

As the renormalization procedure cranks on with this addition to the the source term will acquire corrections and the correlation function will be *generated* (and continually modified with increasing RG step $l$) giving

$$S(\bar{\phi}, \phi, h)_{\Lambda(l)} = S(\bar{\phi}, \phi_{\Lambda(l)}) + \sum_{\delta q} \left( z_\delta(l, q) \Delta_\delta(q) h^*_\delta(q) + \text{h.c.} \right) - \chi_\delta(l, q) h^*_\delta(q) h_\delta(q) + \ldots \tag{2.22}$$

$z_\delta(l, q)$ is a general function that appears after continual renormalization. The correlation function $\chi_\delta(l, q)$ aslo continually changes under the renormalization procedure. A diagrammatic representation of the process is given in Fig. 2.4. General differential equations for the 2-point vertex function and the correlation function are

$$\frac{d}{dl} \ln z = \frac{1}{2} g_\delta \tag{2.23a}$$

$$\frac{d}{dl}\ln\chi_\delta = g_\delta \tag{2.23b}$$

where $g_\delta$ is a combination of terms from the g-ology that can contract with the free legs of the vertex diagram. It is straight forward to see how a divergence in the combination couplings from the g-ology that make up $g_\delta$ will lead to a divergence in the correlation corresponding to a particular order parameter (indicated by the subscript $\delta$).

# Chapter 3

# The 1D-2D Mixed Fermi System

## 3.1 The Model

In a previous chapter I explained how cold atom systems can be engineered to produce a wide array of simulated Bravais lattices by utilizing laser and magnetic trapping and cooling. Additionally, inter-atom interactions can be finely tuned via Feshbach resonances. With these rich and highly tunable robust features, cold atom systems may, in fact, lead to experimental verification of condensed matter phenomena previously only hypothesized theoretically.

In what follows we've imagined an experiment can be constructed which brings into contact two separate species of fermionic atoms which are distinguishable from each other: species $A$ and species $B$. Species $A$ exists on a 1-dimensional lattice engineered as described previously. $A$-atoms can hop from site to site with a hopping strength $t_A$, and two $A$-atoms (with opposing spin) may occupy the same lattice site at the cost of a repulsive energy $U_A$. Similarly, species $B$ is constrained to a 2-dimensional square lattice. $B$-atoms can hop around the sites of the square lattice with hopping strength $t_B$ and, like the 1-dimensional counterpart, incur an energy penalty of $U_B$ when two adjacent

$B$-atoms hop onto the same square lattice site. Additionally, the 1-dimensional lattice is "embedded" into one of the rows of the 2-dimensional lattice in such a way that the $A$ and $B$ atoms can hop onto the same site. Since the $A$ and $B$ atoms are distinguishable, the Hilbert spaces of the two sub-systems are disjoint, and therefore an $A$ and $B$ atom may hop onto the same 1-dimensional lattice site with either spin alignment. Both systems are taken as having a lattice spacing $a$. While in principle the 2-dimensional system could have different horizontal and vertical spacings, they are taken to be the same $a_x = a_y = a$. However, without loss of generality, this lattice spacing is set to unity: $a = 1$.

Both of these subsystems can be described by a Hubbard model [26], each of the energetic parameters completely controllable in the laboratory. The second-quantized Hamiltonian of the system is given by

$$\hat{H} = \hat{H}_A + \hat{H}_B + \hat{H}_I \tag{3.1}$$

where $\hat{H}_A$, $\hat{H}_B$, and $\hat{H}_I$ are the Hamiltonians of the 1D, 2D, and interactions between 1D and 2D systems, respectively, given by

$$\begin{aligned}\hat{H}_A &= t_A \sum_{x,\sigma} c^\dagger_{A,\sigma}(x) c_{A,\sigma}(x+a) + \text{h.c.} \\ &\quad + \frac{U_A}{2} \sum_{x,\sigma} c^\dagger_{A,\sigma}(x) c^\dagger_{A,-\sigma}(x) c_{A,-\sigma}(x) c_{A,\sigma}(x)\end{aligned} \tag{3.2a}$$

$$\begin{aligned}\hat{H}_B &= t_B \sum_{\vec{x},\sigma,i} c^\dagger_{B,\sigma}(\vec{x}) c_{B,\sigma}(\vec{x}+\vec{R}_i) + \text{h.c.} \\ &\quad + \frac{U_B}{2} \sum_{\vec{x},\sigma} c^\dagger_{B,\sigma}(\vec{x}) c^\dagger_{B,-\sigma}(\vec{x}) c_{B,-\sigma}(\vec{x}) c_{B,\sigma}(\vec{x})\end{aligned} \tag{3.2b}$$

$$\hat{H}_I = U_I \sum_{x,\sigma,\sigma'} c^\dagger_{A,\sigma}(x) c_{A,\sigma}(x) c^\dagger_{B,\sigma'}(x,0) c_{B,\sigma'}(x,0) \tag{3.2c}$$

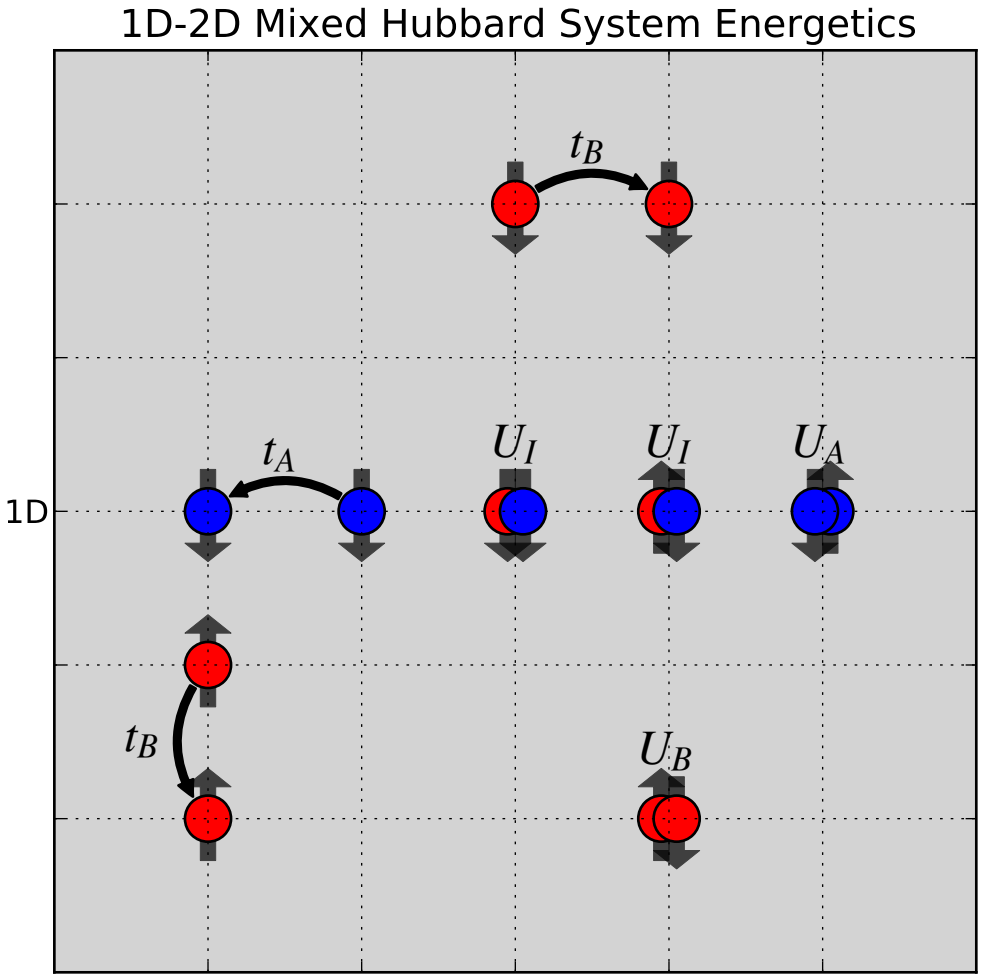


Figure 3.1: Diagram illustrating the physics of the 1D-2D mixed dimensional system. $A$-fermions (blue) can hop between neighboring sites with strength $t_A$ and incur an energy penalty $U_A$ when occupying the same site (with opposing spins). $B$-fermions (red) behave similarly but may move in two dimensions. $A$ and $B$ fermions my occupy the same site (with any spin configuration) at a cost of energy $U_I$

Indeed this is a simplified version of the most general model, constraining the physics to that of nearest neighbors. In essence the Hubbard model is a simplification of a more general tight-binding model where fermions may "hop" beyond neighboring atoms insofar as there is a non-zero overlap between localised wave-functions from any two lattice sites. Thus, the hopping parameter is a relaxed version of the more fundamental hopping integral, akin to the replacement $t(x, x') \to t$. The coupling strength of the interaction term has also been simplified, $U(x_4, x_3; x_1, x_2) \to U$, limiting the interactions to either on-site repulsion or attraction. Lastly, the localized states are reduced to a single band, equivalent to tuning the lattice parameters such that a single one-particle level on each site is isolated from the rest.

The focus of this work is to determine the zero-temperature collective phase of the system which begins with constructing the many-body path integral partition function [5, 46]

$$\mathcal{Z} = e^{-\beta\Omega} = \mathrm{Tr}\ e^{-\beta(\hat{H}-\mu\hat{N})} = \int \mathcal{D}\big[\bar{\phi}\phi\big]\, e^{-S(x,\tau)} \tag{3.3}$$

where the action, $S(x, \tau)$ is given by

$$S(x,\tau) = \sum_i \int_0^\beta d\tau \left[\bar{\phi}_i(\tau)\partial_\tau\phi_i(\tau) + \hat{H}(\bar{\phi}_i(\tau)\bar{\phi}_i(\tau)) - \mu\hat{N}(\bar{\phi}_i(\tau)\bar{\phi}_i(\tau))\right] \tag{3.4}$$

and $\bar{\phi}_i(\tau)$ ($\phi_i(\tau)$) is shorthand for the creation(annihilation) operators replaced by Grassman fields by taking the trace with respect to fermionic coherent states. $\Omega$ is the grand canonical thermodynamic potential $\Omega = \langle\hat{H}\rangle - TS - \mu\mathcal{N}$ [14]. In this sense the system is regarded as being connected to a particle reservoir allowing for, in principle, an infinite number of particles. However, a fixed particle system is achieved by imposing the constraint

$$\mathcal{N} = \langle \hat{N} \rangle = \mathrm{Tr} \sum_{x,\sigma} c_\sigma^\dagger(x) c_\sigma(x) e^{-\beta(\hat{H}-\mu\hat{N})} \tag{3.5}$$

which amounts to fixing the chemical potential $\mu$ [4].

The most convenient set of single particle states to work in are those in which the kinetic (or one-body) term is diagonal. The basis used to write the Hamiltonian in 3.2 is the Wannier basis [68, 69], and in the simplified, single-band restriction of the basis there are two states for every lattice site in the system (namely $|x,\uparrow\rangle$ and $|x,\downarrow\rangle$), where the total number of lattice sites in the system is denoted by $\mathcal{N}$. Diagonalising the two-body term is achieved by Fourier transforming from the Wannier states to the Bloch states. For added convenience in evaluating various physical quantities, an additional Fourier transform is made from the imaginary "time" $\tau$ to the Matsubara Frequency $\omega_n$ [3]. This results in the replacement of the fields

$$\phi_\sigma(\vec{x},\tau) = \frac{1}{\sqrt{N\beta}} \sum_{\vec{k}}^{B.Z.} \sum_{\omega_n} e^{i(\vec{k}\cdot\vec{x}-\omega_n\tau)} \phi_\sigma(\vec{k},\omega_n) \tag{3.6}$$

where, due to the anti-commuting nature of the fermionic creation/annihilation operators (Grassman numbers) the Matsubara frequencies are $\omega_n = (2n+1)\pi/\beta$ with $n = 0, \pm1, \pm2, \ldots$. With these substitutions, the action takes the form in which each of the one-body terms are diagonal

$$S_A = \sum_{k,\omega,\sigma} \bar{\phi}_\sigma(k\omega)[-i\omega + \epsilon_A(k) - \mu_A]\phi_\sigma(k\omega) +$$
$$\frac{U_A}{2N\beta} \sum_{\{k\omega\},\sigma} \bar{\phi}_\sigma(k_4\omega_4)\bar{\phi}_{-\sigma}(k_3\omega_3)\phi_{-\sigma}(k_2\omega_2)\phi_\sigma(k_1\omega_1)\bar{\delta}(k_1+k_2-k_3-k_4)\delta(\omega_1+\omega_2-\omega_3-\omega_4) \tag{3.7a}$$

$$S_B = \sum_{\vec{p},\Omega,\sigma} \bar{\Phi}_\sigma(\vec{p}\Omega)[-i\Omega + \epsilon_B(\vec{p}) - \mu_B]\Phi_\sigma(\vec{p}\Omega) +$$
$$\frac{U_B}{2N^2\beta} \sum_{\{\vec{p},\Omega\},\sigma} \bar{\Phi}_\sigma(\vec{p}_4\Omega_4)\bar{\Phi}_{-\sigma}(\vec{p}_3\Omega_3)\Phi_{-\sigma}(\vec{p}_2\Omega_2)\Phi_\sigma(\vec{p}_1\Omega_1)\bar{\delta}(\vec{p}_1+\vec{p}_2-\vec{p}_3-\vec{p}_4)\delta(\Omega_1+\Omega_2-\Omega_3-\Omega_4) \tag{3.7b}$$

$$S_I = \frac{U_I}{N^2\beta} \sum_{\substack{k,k',\sigma \\ \vec{p},\vec{p}',\sigma'}} \bar{\phi}_\sigma(k\omega)\bar{\phi}_\sigma(k'\omega')\bar{\Phi}_{\sigma'}(\vec{p}\Omega)\bar{\Phi}_{\sigma'}(\vec{p}'\Omega')\bar{\delta}(k+p_x-k'-p'_y)\delta(\omega+\Omega-\omega'-\Omega') \tag{3.7c}$$

and the 1D/2D dispersions are given by

$$\epsilon_A(k) = -2t_A\cos(k) \tag{3.8a}$$

$$\epsilon_B(\vec{p}) = -2t_B\left(\cos(p_x) + \cos(p_y)\right) \tag{3.8b}$$

Up until now the interactions in the two-dimensional system have been included in the model. In what follows, however, they will be dropped. This is equivalent to a one dimensional fermionic Hubbard system interacting with a two-dimensional "lattice gas." This simply refers to an action (or Hamiltonian) with a two-body term only, and describes $B$-fermions moving freely on the square lattice, but with a dispersion given by 3.8b. The notation $\bar{\delta}$ means momentum is conserved *up to* multiples of $2\pi$ which will play a crucial roll in the Renormalization Group treatment to follow.

The interaction term between systems $A$ and $B$ reveals important information

about the symmetry of the combined system. As can be seen from the momentum conserving delta function in the inter-system interaction term in 3.7, momentum is only conserved in the $x$-direction. This is an artifact of translational symmetry in the $x$-direction, but no translational symmetry in the $y$-direction.

## 3.2 The Mediated Interaction

The action of 3.7 is the starting point of obtaining an effective model for the 1D system. By constructing the partition function of the entire system and carrying out the partial sum over *only* the fast 2D Grassman fields $(\bar{\Phi}, \Phi)$, an effective model describing the physics in 1D is achieved. The resulting model is different from the original model in that a new interaction, dubbed $U_{eff}$, contains the effects of 1D fermions due to scatterings events involving processes where two $A$-fermions scatter into two $B$-fermions which eventually scatter into two more $A$-fermions.

The $A$-$B$ partition function has the schematic form

$$\mathcal{Z} = \int \mathcal{D}_A e^{-S_A} \int \mathcal{D}_B e^{-(S_B+S_I)} \tag{3.9a}$$

$$= \mathcal{Z}_B \int \mathcal{D}_A e^{-S_A} \langle e^{-S_I} \rangle_B \tag{3.9b}$$

$$= \int \mathcal{D}_A e^{-(S_A + \ln\langle e^{-S_I}\rangle_B - \ln \mathcal{Z}_B)} \tag{3.9c}$$

$$= \int \mathcal{D}_A e^{-S_{eff}} \tag{3.9d}$$

In 3.9d the effective action has been identified as the remnants from the original action after all $B$-fermions have been explicitly summed over. The expression $\langle e^{-S_i} \rangle_B$ denotes the many-particle statistical average with respect to the $B$-fermions only. By re-exponentiating this term, the contribution to the effective action comes from the

evaluation of the expression $\ln\langle e^{-S_I}\rangle_B$. In doing so, the so-called "cumulant expansion" [2, 32] is used. As with the 1D on-site interactions, the density-density inter-species interaction strength, $U_I$, is taken to be weak. Thus, it is sufficient to keep only terms up to order $U_I^2$.

The expansion is defined as

$$\ln\langle e^{-S_I}\rangle_B = \sum_{n=1}^{\infty} \frac{(-1)^n}{n!}\langle S_I^n\rangle_{B,con.} \tag{3.10}$$

where $\langle X\rangle_{con.}$ denotes a "connected" average. The $n = 1$ term in the sum is trivially connected, while for $n \geq 2$ this implies the terms in the Wick's theorem [19] expansion cannot be factored into multiples of $\langle S_I\rangle$. Up to $n = 2$ the effective action becomes

$$S_{eff} = S_A + \langle S_I\rangle_B - \frac{1}{2}\langle S_I^2\rangle_{B,con.} - \ln\mathcal{Z}_B \tag{3.11}$$

The term $\ln\mathcal{Z}_B$ is simply a constant logarithmic correction and can be dismissed. $\langle S_I\rangle_B$ contains two $A$-fermion fields and thus modifies the existing two-body terms. Evaluating this term gives

$$\langle S_I\rangle_B = -\frac{2U_I}{N^2\beta}\sum_{k,\omega}\sum_{\vec{p},\Omega}\mathcal{G}_B(\vec{p};\Omega)\bar{\phi}_\sigma(k\omega)\bar{\phi}_\sigma(k\omega) \tag{3.12a}$$

$$= -U_I\nu_B\bar{\phi}_\sigma(k\omega)\bar{\phi}_\sigma(k\omega) \tag{3.12b}$$

where $\mathcal{G}_B(\vec{p};\Omega)$ is the 2D Green function $1/(-i\Omega + \epsilon_B(\vec{p}) - \mu_B)$ and $\nu_B$ represents the fraction of particles with energy less than the 2D chemical potential. This term is diagonal in $k, \omega$ and is simply absorbed into a new definition of the chemical potential

$$\mu'_A = \mu_A + U_I\nu_B \tag{3.13}$$

The next highest order term is proportional to $U_I^2$ and involves only connected contractions of $\langle \Phi_\sigma(\vec{p}_1'\Omega_1')\Phi_{\sigma'}(\vec{p}_2'\Omega_2')\bar{\Phi}_\sigma(\vec{p}_1\Omega_1)\bar{\Phi}_{\sigma'}(\vec{p}_2\Omega_2)\rangle$. Being proportional to four $A$-fermion fields, this term represents an effective 1D interaction of the $A$-fermions, mediated through scattering processes involving $B$-fermions. Evaluation of the mediated two-body term goes as

$$\langle S_I(1)S_I(2)\rangle_{con.} =$$
$$\frac{-1}{N\beta}\sum_{\{k\omega\}\sigma\sigma'} U_{eff}(k_4,k_3;k_1,k_2)\bar{\phi}_\sigma(4)\bar{\phi}_{\sigma'}(3)\phi_{\sigma'}(2)\phi_\sigma(1)\bar{\delta}(k_1+k_2-k_3-k_4)\delta(\omega_1+\omega_2-\omega_3-\omega_4) \tag{3.14}$$

$U_{eff}(\{k,\omega\})$ is a function of the momenta and Mtsubara frequencies of a two $A$-particle scattering event "mediated" by $B$-fermions that have found their way onto the 1D line and is given by

$$U_{eff}(\{k,\omega\}) = \frac{2U_I^2}{N^3\beta}\sum_{\vec{p},q,\Omega}\mathcal{G}_B(\vec{p};\Omega)\mathcal{G}_B(p_x+k_{41},q;\Omega+\omega_{41}). \tag{3.15}$$

$k_{41}$ ($\omega_{41}$) is shorthand for $k_4-k_1$ ($\omega_4-\omega_1$), the momentum (Matsubara frequency) difference between $A$-fermions 4 and 1.

The effective action for the purely 1D $A$-fermions can now be written as follows

$$\begin{aligned} S_{eff} = &\sum_{k,\omega,\sigma}\bar{\phi}_{A,\sigma}(k\omega)\left[-i\omega+\epsilon_A(k)-(\mu_A+U_I\nu_B)\right]\phi_{A,\sigma}(k\omega) \\ &+\frac{1}{2}\sum_{\{k\omega\}\sigma}\left[U_A+U_{eff}(4,3;1,2)\right]\bar{\phi}_\sigma(4)\bar{\phi}_{-\sigma}(3)\phi_{-\sigma}(2)\phi_\sigma(1)\delta(1+2-3-4) \\ &+\frac{1}{2}\sum_{\{k\omega\}\sigma}U_{eff}(k_4,k_3;k_1,k_2)\bar{\phi}_\sigma(4)\bar{\phi}_\sigma(3)\phi_\sigma(2)\phi_\sigma(1)\delta(1+2-3-4) \end{aligned} \tag{3.16}$$

The appearance of the numbers $1-4$ in the terms above is a shorthand for momenta and

Matsubara frequencies with those indices. To further evaluate the effective interaction coupling in 3.15 requires a technique for carrying out Matsubara sums of the form

$$\frac{1}{\beta}\sum_{\omega_n} f(\omega_n) \tag{3.17}$$

with a clever techniqe that involves dreaming up a contour integral whose sum of residues results in the Matsubara sum in question [35]. This leaves the effective interaction in the form

$$\frac{2U_I^2}{N^3}\sum_{\vec{p},q}\frac{n[\epsilon_B(p_x+k_{41},q)]-n[\epsilon_B(p_x,p_y)]}{i\omega_{41}+\epsilon_B(p_x+k_{41},q)-\epsilon_B(p_x,p_y)} \tag{3.18}$$

in which the momentum and Matsubara frequencies of the $A$-fermions appear only in the differences $k_4-k_1$ and $\omega_4-\omega_1$. Here, $n(\epsilon)$ is the familiar fermi-function $1/(e^{\beta(\epsilon-\mu)}+1)$. The frequency dependence is often referred to as "retardation" and is a common occurrence in problems of fermions coupling to lattice phonons [34]. In what follows retardation effects of the problem will be ignored. Additionally, the difference of momenta 4 and 1 in $U_{eff}$ is an indicator of translational invariance in the $x$-direction of the system.

By taking the thermodynamic limit of the sum and utilizing the transformation $1/N\sum_k f(k) \to \int_{B.Z.} dk/2\pi f(k)$, $U_{eff}$ becomes solvable by numerical integration techniques. The present work uses a Monte Carlo integration routine available through the Python "skmonaco" package. The effective interaction as a function of $k_4-k_1$ is depicted in 3.2 for $0 < \mu_b < 4t_B$. The function is symmetric with respect to positive and negative chemical potential. As seen from the figure, the form of the function changes as $\mu_B$ varies, but remains negative for all values within the Brillouin zone. As will be more important in the Renormalization Group analysis to follow, the relative

values of the mediated interaction for momentum transfers of zero and $\pi$ ($U_{eff}(0)$ and $U_{eff}(\pi)$) vary as the 2D filling (or, equivalently, $\mu_B$) ranging from $|U_{eff}(0)| > |U_{eff}(\pi)|$ to $|U_{eff}(0)| \sim |U_{eff}(\pi)|$ to $|U_{eff}(0)| < |U_{eff}(\pi)|$.

Up until now the mediated interaction has been represented in the Bloch basis states. By performing the inverse transformation of 3.6 (neglecting the Matsubara frequency transformation) the mediated interaction in the Wannier basis is recovered. This gives a direct reflection of the behavior the mediated interaction in the physical space of the lattice. With this transfer of basis $U_{eff}$ becomes

$$U_{eff}(x) = \frac{1}{N} \sum_{k_{41}}^{B.Z.} e^{-ik_{41}x} U_{eff}(k_{41}) \tag{3.19}$$

A summary of the behavior for $U_{eff}(x)$ can be seen in Fig. 3.3 where $x$ can be thought of as the difference in position of two interacting particles. For simplicity, one particle is centered at $x = 0$ and the other particle can sit at one of 100 neighboring lattice sites. For each value of $\mu_B$ the second particle experiences an attraction if it finds itself at $x = 0$ (with opposing spin to the original particle). As $\mu_B$ varies, a second particle on the nearest neighboring site will experience an interaction which varies from repulsion to attraction. This interaction damps out to zero from the next-nearest neighboring site on to the rest of the sites on the lattice which is concurrent with the prescription that the interaction be "weak."

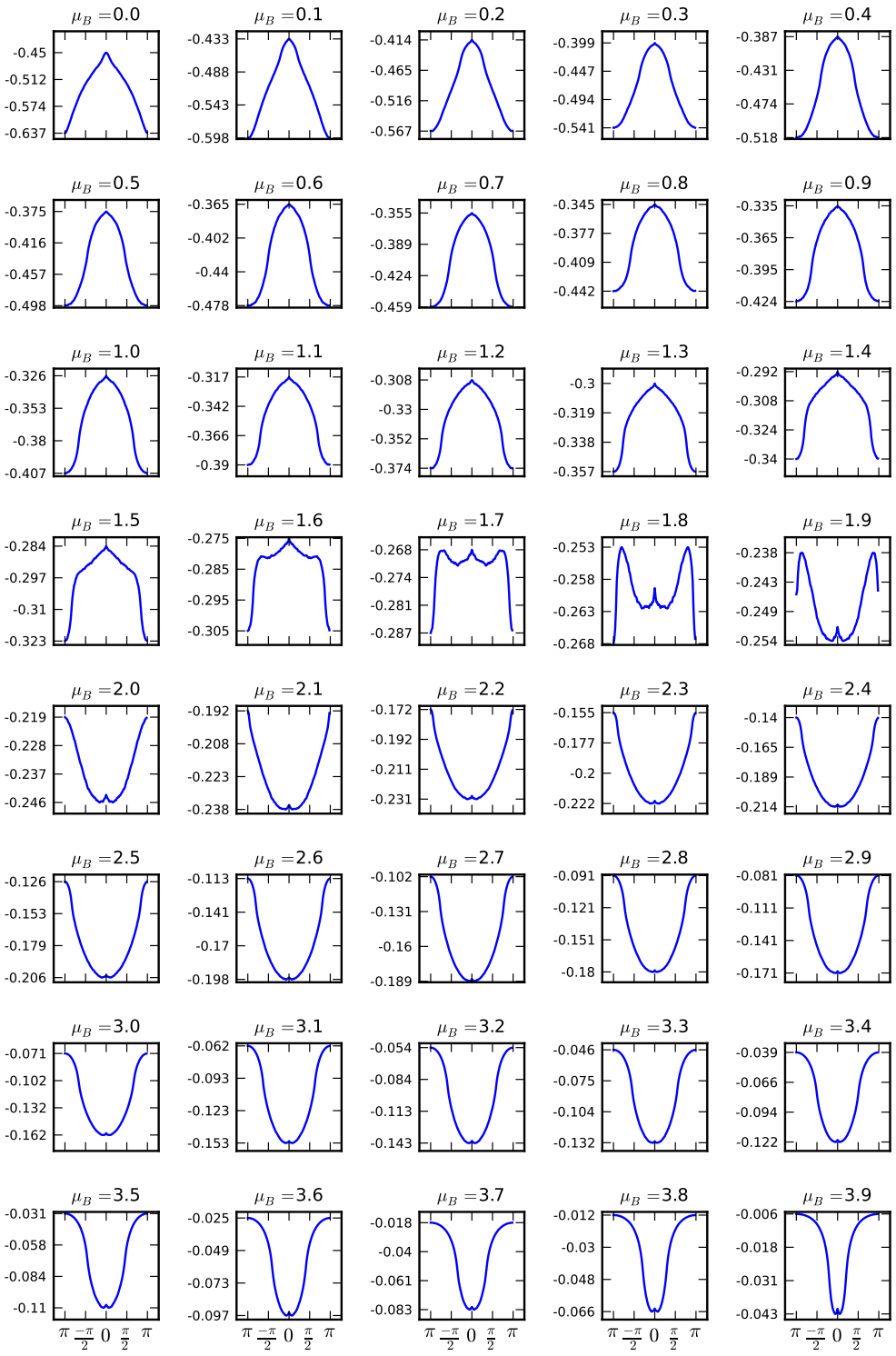


Figure 3.2: $U_{eff}(k_{41})$ for positive values of the 2D chemical potential

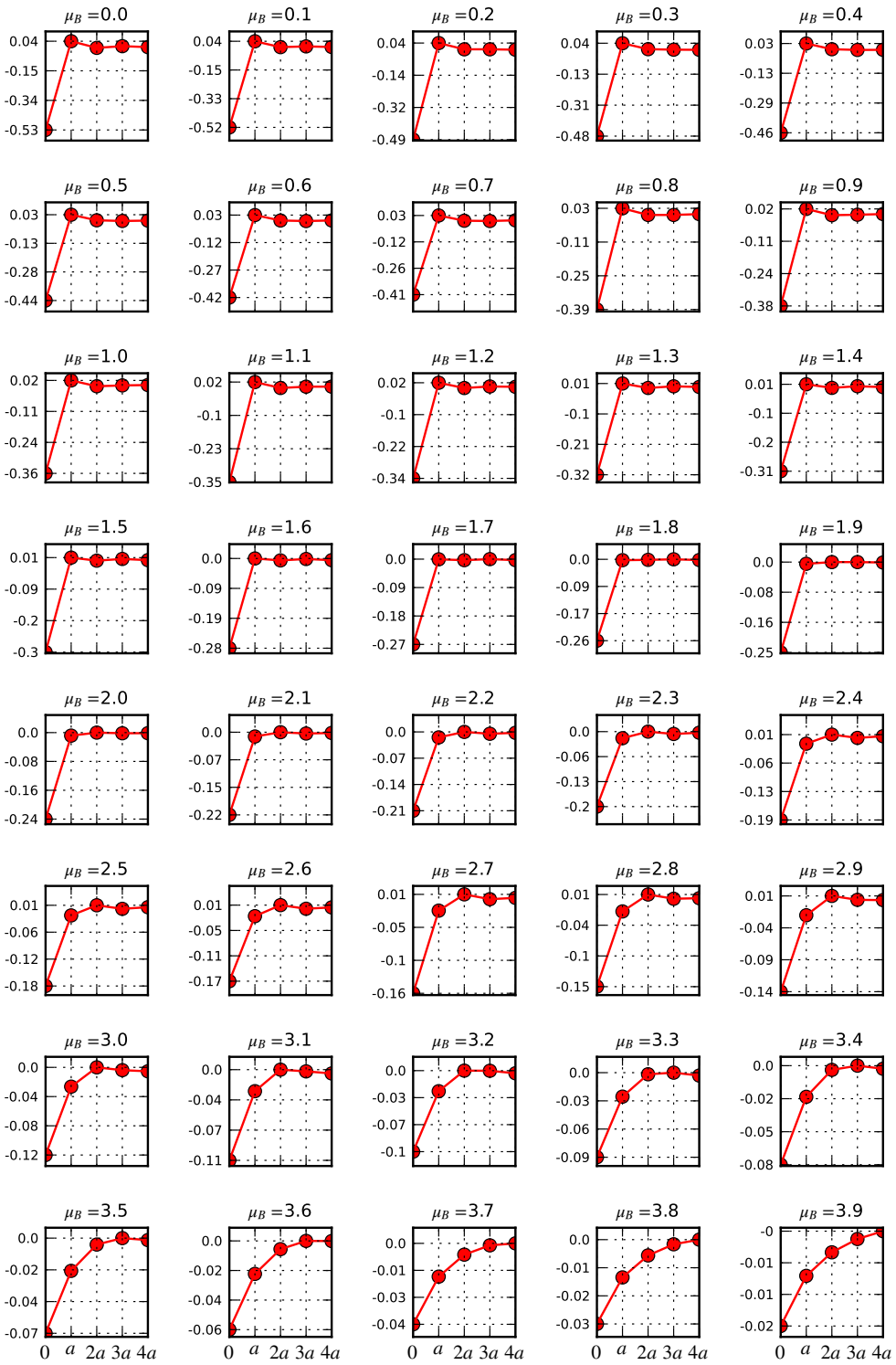


Figure 3.3: $U_{eff}(x)$ for positive values of the 2D chemical potential

## 3.3 Results of the Renormalization

In the previous section the flow equations for the four unique scatterings, denoted by the g-ology, were obtained. It was shown that a divergence of particular combinations of g-ology couplings is accompanied by a divergence of a correlation function corresponding to a particular order parameter. To determine the phase of the effective one-dimensional system at hand, it is necessary to solve the flows of Eq.(2.19). The initial conditions of the flows correspond to the values of the interaction before the renormalization process started, i.e. $S(\bar{\phi}, \phi)^{l=0}$.

Referring to the diagrams for the g-ology scatterings in Fig.2.3, it is seen that the momentum transfer between particles 1 and 4 is $\pm\pi$ for $g_1, g_3$ and 0 for $g_2, g_4$. Thus the initial conditions to the flows of $g_1 \ldots g_4$ are

$$g_1^{l=0} = g_3^{l=0} = U_A + U_{eff}(k_{41} = \pi) \tag{3.20a}$$

$$g_2^{l=0} = g_4^{l=0} = U_A + U_{eff}(k_{41} = 0). \tag{3.20b}$$

Fig. 3.2 shows the effective interaction as a function of $k_4 - k_1$ for various values of the two-dimensional chemical potential. Since the relative values of $U_{eff}(0)$ and $U_{eff}(\pi)$ are fixed by fixing $\mu_B$, the zero-temperature quantum phase is essentially controlled by the two-dimensional density. The phase diagram of the system is thus parameterized in the space of $|U_{eff}(0)|$ and $|U_{eff}(\pi)|$.

The prescription for determining the phase for the mixed one-dimensional/ two-dimensional system goes as follows:

- fix the two-dimensional chemical potential
- simultaneoulsy solve the flow equations for the g-ology couplings and the correla-

| Phase | Order Parameter | 1D Coupling |
|---|---|---|
| $\mathrm{CDW}_\pi$ | $\sum_\alpha \bar{\phi}_\alpha(k)\phi_\alpha(k+\pi)$ | $g_2 - 2g_1 \mp g_3$ |
| $\mathrm{SDW}_\pi$ | $\sum_i \sum_{\alpha,\beta} \bar{\phi}_\alpha(k)\sigma^i_{\alpha\beta}\phi(k+\pi)$ | $g_2 \pm g_3$ |
| $\mathrm{SS}_0$ | $1/\sqrt{2}\sum_\alpha \alpha\phi_\alpha(k)\phi_\alpha(-k)$ | $-g_1 - g_2$ |
| $\mathrm{ST}_0$ | $\sum_\alpha \left(1/\sqrt{2}\phi_\alpha(k)\phi_{-\alpha}(-k) + \phi_\alpha(k)\phi_\alpha(-k)\right)$ | $g_1 - g_2$ |

Table 3.1: Parameters for various one-dimensional phases and the g-ology couplings that influence the renormalization of the correlation functions. The subscript indicates the momentum in the particle-hole (CDW/SDW) and particle-particle (SS/ST) channels.

tion functions

- check the couplings and correlations for divergences to determine the dominant phase of the system
- if no correlations diverge, the phase corresponds to the largest correlation function at long renormalization step values.

The phase diagram for the 1D/2D mixed dimensional system is shown in Fig. 3.4. The topology is typical of one-dimensional SU(2) symmetric interacting fermi systems, and is divided into distinct regions where particular couplings diverge due to the divergence of the g-ology couplings. These special couplings derive from the partitioning of the most general SU(2) symmetric interaction into charge-spin and singlet-triplet components. Following the renormalization of these components involves renormalizing the combination of g-ology couplings given in the third column of Table 3.1.

The most generic SU(2) symmetric interaction can be partitioned into distinct pieces as

$$S_I = \sum_{kk'q} U_c(k,k',q)\bar{\Delta}_q^{\mathrm{CDW}}(k)\Delta_q^{\mathrm{CDW}}(k') + U_\sigma(k,k',q)\bar{\Delta}_q^{\mathrm{SDW}}(k)\Delta_q^{\mathrm{SDW}}(k') \tag{3.21a}$$

$$S_I = \sum_{kk'q} U_{\mathrm{SS}}(k,k',q)\bar{\Delta}_q^{\mathrm{SS}}(k)\Delta_q^{\mathrm{SS}}(k') + U_{\mathrm{ST}}(k,k',q)\bar{\Delta}_q^{\mathrm{ST}}(k)\Delta_q^{\mathrm{ST}}(k') \tag{3.21b}$$

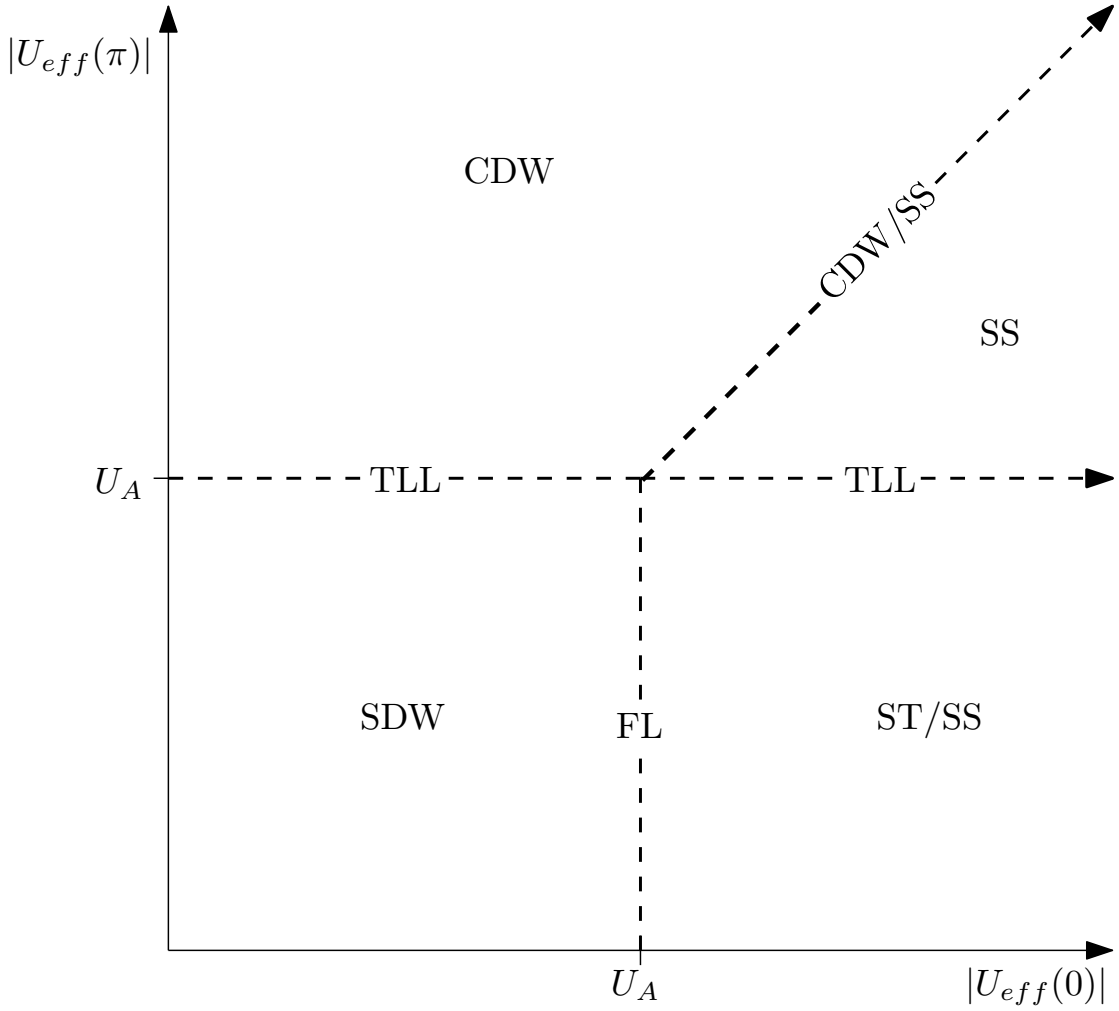


Figure 3.4: Phase diagram for the 1D/2D mixed dimensional system. The CDW, SDW, CDW/SS (single line), regions correspond to diverging correlations. The TLL lines indicate $g_1, g_3 \to 0$ and $g_2, g_4$ remain constant, signaling Tomonaga-Luttinger behavior. The FL (fermi liquid) line corresponds to all g-ology couplings renormalizing to zero from non-zero values. The lower left region sees decaying correlations where ST decays the slowest followed by SS.

where the order parameters of interest are given in the second column of Table 3.1. As can be seen from the table, the focus is on momenta of $\pm\pi$ for particle-hole couplings and of zero for particle- particle couplings.

Fig. 3.6a shows enhancement of the SDW coupling due to a divergence of the Umklapp and forward scatterings, while the back scattering and $g_4$ couplings remain at zero in the region with $|U_{eff}(\pi)|$, $|U_{eff}(0)| < |U_A|$. As $U_{eff}(\pi)$ approaches the line $|U_{eff}(\pi)| = |U_A|$, the Umklapp and back scattering terms remain at zero while the forward and $g_4$ terms remain at a constant positive value as in Fig. 3.6e. A model with only $g_2$ and $g_4$ may be recast and described by the Tomonaga-Luttinger model [65, 42, 24]. As the line is crossed into the region with $|U_{eff}(\pi)| > |U_A|$, the forward scattering diverges to positives values again, but the Umklapp scattering diverges to negative values as seen in Fig. 3.6b. This leads to an enhancement and dominance of the CDW coupling. The CDW phase persists in the region until crossing the line $|U_{eff}(\pi)| = |U_{eff}(0)|$ with both $|U_{eff}(\pi)|$, $|U_{eff}(0)| > |U_A|$. At this boundary the back and forward scattering diverge to negative values while the Umklapp and $g_4$ terms start and remain at zero. Here the CDW and SS couplings diverge equally and simultaneously as indicated in Fig. 3.6c. As this boundary is crossed, the SS coupling is enhanced and dominates. When $|U_{eff}(0)| = |U_A|$ and $|U_{eff}(\pi)| < |U_A|$ the backward and Umklapp scatterings flow to zero while the forward and $g_4$ scatterings start and remain at zero as seen in Fig.3.6f. Thus, the renormalized system is one in which the interactions have vanished which is precisely the definition of a fermi liquid. precisely the description of a fermi liquid and

In the region where $|U_{eff}(0)| > |U_A|$ and $|U_{eff}(\pi)| < |U_A|$ no couplings diverge. The backward and Umklapp couplings start out at non-zero positive initial values but quickly renormalize to zero. $g_4$ starts at a negative value and remains at that constant

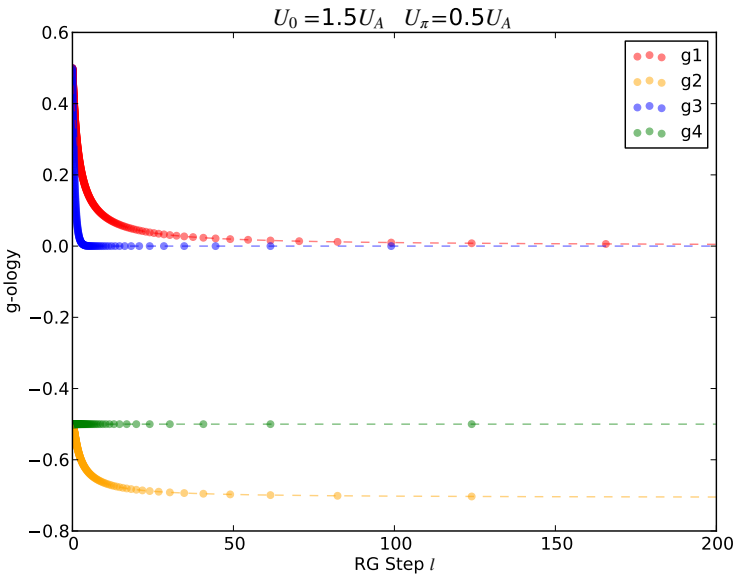


Figure 3.5: Renormalization of the g-ology couplings in the region of the phase diagram where $|U_{eff}(0)| > |U_A|$ and $|U_{eff}(\pi)| < |U_A|$

negative value. The forward scattering starts at a negative value and renormalizes to another more-negative value and remains constant as the renormalization cranks on. This behavior is shown in Fig.3.3. The system can be bosonized and recast in the language of the Tomonaga-Luttinger model. The behavior here is similar to the behavior at the TLL line in the phase diagram except that the couplings start out at non-zero values and change as discussed previously rather than starting and remaining constant. Since no couplings diverge, there isn't a truly long-range order as when the correlations diverge like in the other regions of the phase diagram. In this case, the phase of the system is quoted as owing to the correlations which decay the slowest in a bosonized version of the system [45]. Here, the ST correlations are the slowest decaying followed by the SS correlations.

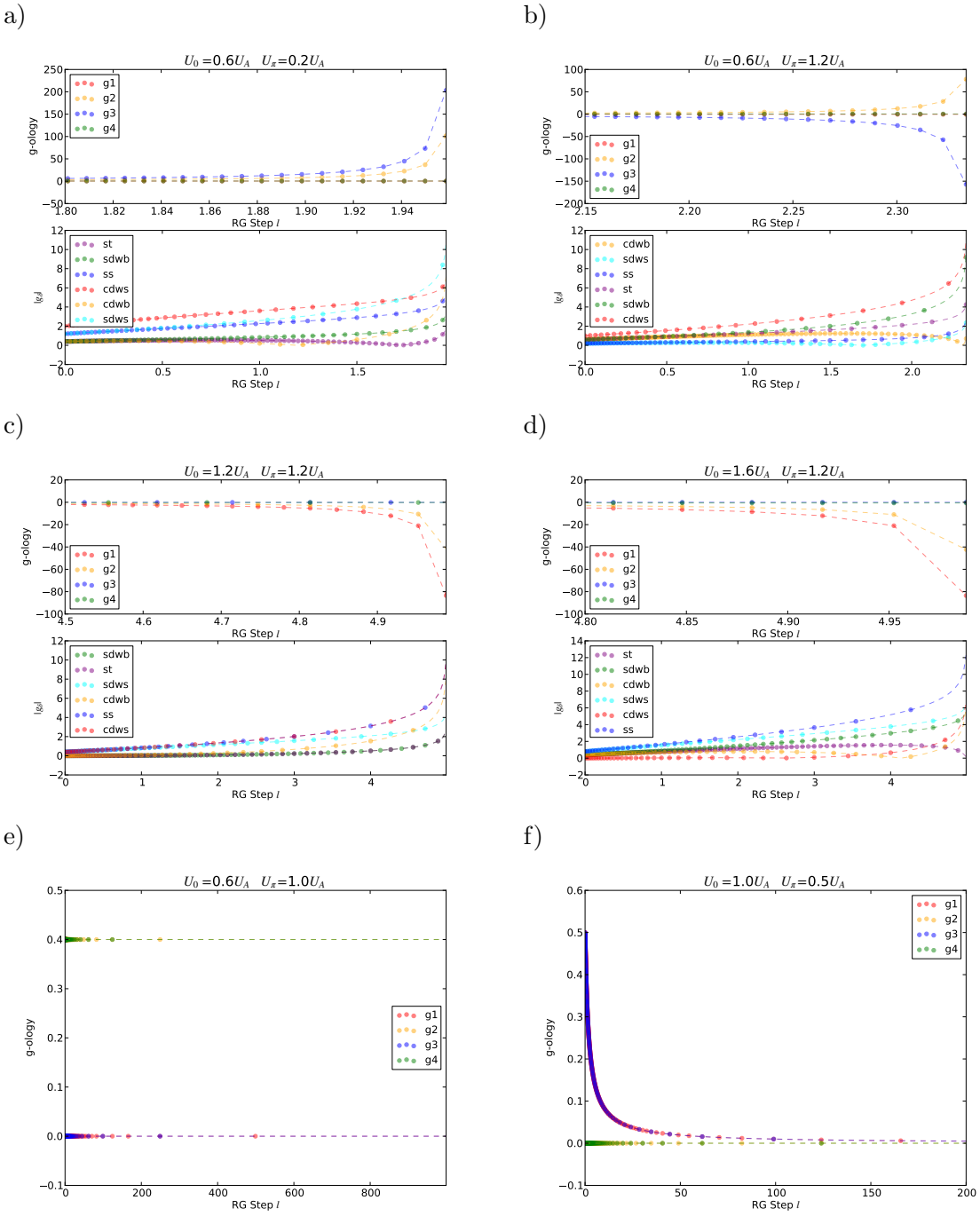


Figure 3.6: a), b), c), and d) show the behavior of the g-ology couplings accompanied by divergences of couplings associated with CDW, SDW, SS, and ST interactions. e) shows $g_1$,$g_3$ starting (and remaining) at zero while $g_2$,$g_4$ remain constant. f) shows all g-ology couplings either remaining or renormalizing to zero suggesting a fermi liquid.

# Chapter 4

# Phase-Manipulation of a Two-Leg Ladder in Mixed Dimensions

## 4.1 Introduction

In the previous chapter a 1D-2D mixed dimensional system was considered. In what follows, this idea is extended to a two-leg ladder embedded into 2D square lattice; in this vein the system of the previous chapter could be considered a "one-leg" ladder. This is study a mixed-dimensional two-species fermionic system: one species confined in a two-leg ladder with on-site repulsion, the other moving freely in a two-dimensional (2D) square lattice. An inter-species interaction is also introduced as on-site due to the energy cost of double occupation. Integrating out the 2D fermionic gas, a mediated long-range interaction is generated in the ladder. We show that the mediated interaction moves the bare on-site interaction in the two-leg ladder off the symmetric point, and enhances the charge density wave (CDW) instability in the renormalization group (RG) transformation. Here we use the term charge-density-wave to refer to density modulations in analogy with nomenclature used in the study of electronic systems, even

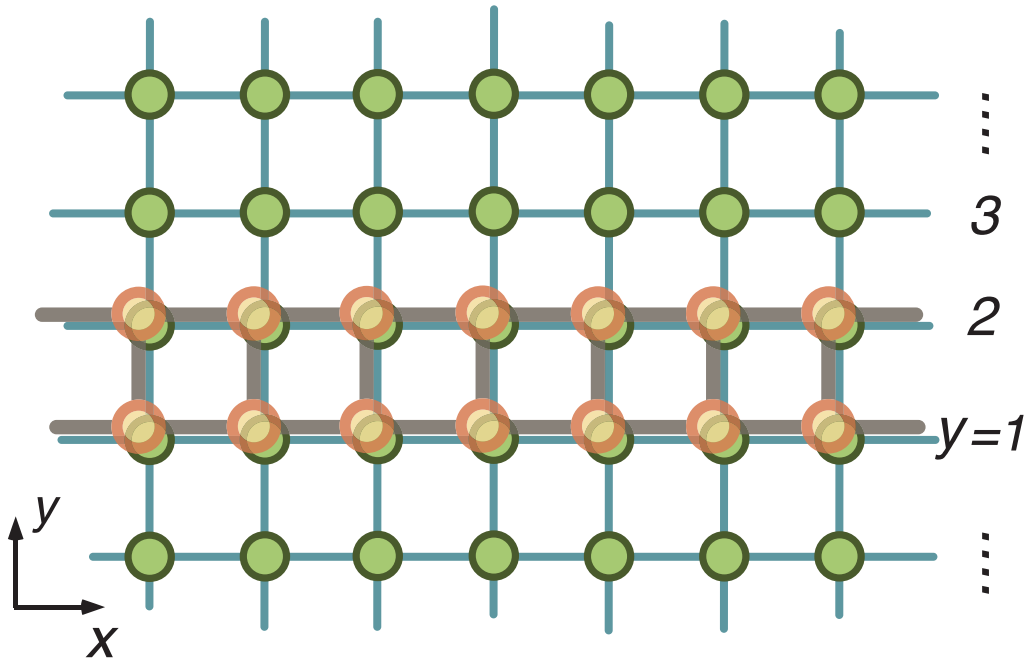


Figure 4.1: A two-leg ladder embedded in a 2D square lattice and the coordinate system are illustrated.

though the atoms are charge neutral. We find that, by controlling the filling in the 2D gas, the phase of the ladder can be tuned. By mapping out the phase diagram for various parameters, we show the possible quantum phase-manipulation of a two-leg ladder in mixed dimensional fermionic cold atoms.

## 4.2 Formalism

A schematic of the system we consider here is illustrated in Fig. 4.1. The action can be written as $S = S_l + S_c^0 + S_{cl}$, where $S_l$ stands for the action for the two-leg ladder with on-site interaction $U_l$. The action of the non-interacting 2D system is denoted as

$$S_c^0 = \int d\tau \sum_{\langle \vec{r},\vec{r}' \rangle} \bar{\phi}_\alpha(\vec{r},\tau) \left[ \partial_\tau \delta_{\vec{r},\vec{r}'} + H_c(\vec{r},\vec{r}') \right] \phi_\alpha(\vec{r}',\tau) \tag{4.1}$$

where $\bar{\phi}_\alpha$,$\phi_\alpha$ are Grassmann fields with (pseudo) spin index $\alpha$, and the Hamiltonian is represented as $H_c(\vec{r},\vec{r}') = \left[t_c(\vec{r},\vec{r}') - \mu_{2D}\delta_{\vec{r},\vec{r}'}\right]$ with chemical potential $\mu_{2D}$. Moreover, the uniform hopping amplitude $t_c(\vec{r},\vec{r}') = -1$ when $\vec{r}$ and $\vec{r}'$ represent nearest neighbor sites. The energy cost of for overlap of two atoms of different species can be regarded as the on-site inter-species repulsion with strength $U_{cl}$ and represented as

$$S_{cl} = \int d\tau U_{cl} \sum_a \sum_{\vec{r}} n_c(\vec{r},\tau) n_l(\vec{r},\tau)\delta_{y,a}, \tag{4.2}$$

where $n_c = \sum_\alpha \bar{\phi}_\alpha(\vec{r})\phi_\alpha(\vec{r})$ and $n_l = \sum_\alpha \bar{\varphi}_{y\alpha}(x)\varphi_{y\alpha}(x)$ are the densities for the 2D lattice and the ladder, respectively. The summation over $a = 1, 2, \cdots, N$ stands for the position of $N$-legs along the $y$-direction, as shown as Fig. 4.1. Here we focus on the $N = 2$ case.

Considering the limit of weak inter-species interactions ($U_{cl}/t_c < 1$), we expand the action in powers of $U_{cl}$ and integrate out the non-interacting 2D gas, neglecting terms $O(U_{cl}^3)$. The first term in the expansion gives a self-energy correction to the chemical potential of the ladder system. Since this only slightly shifts the phase boundaries, we ignore it here. The second term generates a mediated interaction, modifying the profile of the total effective interaction in the two-leg ladder. The action for the ladder can now be written as $S_{\text{eff}} = S_l + S_{\text{med}}$, where

$$S_{\text{med}} \simeq \int d\tau_1 \int d\tau_2 \frac{U_{cl}^2}{2} \sum_{a,b} \delta_{y_1,a}\delta_{y_2,b} \text{tr}\Big[n_l(\vec{r}_1,\tau_1)\mathcal{G}_0(\vec{r}_1,\tau_1;\vec{r}_2,\tau_2) n_l(\vec{r}_2,\tau_2)\mathcal{G}_0(\vec{r}_2,\tau_2;\vec{r}_1,\tau_1)\Big], \tag{4.3}$$

with $\mathcal{G}_0(\vec{r},\tau;\vec{r}',\tau') = \left[\partial_\tau \delta_{\vec{r},\vec{r}'} - H_c(\vec{r},\vec{r}')\right]^{-1}$ the imaginary-time Green's function. This shows that a mediated interaction between particle $n_l(\vec{r}_1,\tau_1)$ and $n_l(\vec{r}_2,\tau_2)$ with retardation effects is generated in the ladder system. Retardation effects can be

neglected when the Fermi velocity of the 2D fermions is large compared with the one for the ladder.

## 4.3 The Mediated Interaction

We now study the effects of the effective interaction on the ladder system and determine its phase diagram using a RG technique. By ignoring retardation effects, the Grassmann number $\varphi$ is decomposed into chiral pairs [6, 39, 40, 15, 10, 11], $\varphi_y(x) \approx \sum_{P,i} T_{yi}\psi_{Pn}(x)e^{iPk_{F_i}x}$, where $P = R/L = +/-$ represent right /left-moving particles, and $k_{F_i}$ is the Fermi wavelength of the band index $i$. The transformation matrix between leg-index $y$ and band-index $i$ in the $N$-ladder is introduced as $T_{yi} = \sqrt{\frac{2}{N+1}}\sin\left[\frac{\pi}{N+1}yi\right]$[39, 40]. The interactions between these chiral fermions can be categorized as Cooper scatterings $c^l_{ij}$, $c^s_{ij}$ and forward scatterings $f^l_{ij}$, $f^s_{ij}$, where we set $f_{ii} = 0$ since $f_{ii} = c_{ii}$. Thus, the mediated interactions in a ladder system can be written as

$$S_{\rm med} \simeq \frac{U_{cl}^2}{U_l}\int d\tau \int dx \Big[ f^s_{ij}\bar{\psi}_{Ri\alpha}\psi_{Ri\alpha}\bar{\psi}_{Lj\beta}\psi_{Lj\beta} + f^l_{ij}\bar{\psi}_{Ri\alpha}\psi_{Lj\alpha}\bar{\psi}_{Lj\beta}\psi_{Ri\beta} + c^s_{ij}\bar{\psi}_{Ri\alpha}\psi_{Rj\alpha}\bar{\psi}_{Li\beta}\psi_{Lj\beta} + c^l_{ij}\bar{\psi}_{Ri\alpha}\psi_{Lj\alpha}\bar{\psi}_{Li\beta}\psi_{Rj\beta}\Big], \tag{4.4}$$

where the bare values of the couplings are expressed as

$$f^s_{ij} = U^{\rm med}_{iijj}(0) \tag{4.5a}$$

$$f^l_{ij} = U^{\rm med}_{ijji}(k_{F_i} + k_{F_j}) \tag{4.5b}$$

$$c^s_{ij} = U^{\rm med}_{ijij}(k_{F_i} - k_{F_j}) \tag{4.5c}$$

$$c^l_{ij} = U^{\rm med}_{ijij}(k_{F_i} + k_{F_j}) \tag{4.5d}$$

with the definition of dimensionless mediated interactions,

$$U_{ijkl}^{\mathrm{med}}(k) = U_l \int_{-\pi}^{\pi} \frac{dq}{2\pi} \Gamma_{ijkl}(q) \chi_0(k,q). \tag{4.6}$$

Here the particle-hole propagator is defined as

$$\chi_0(k,q) = \int \frac{d\vec{p}}{4\pi^2} \frac{n_F\Big[\epsilon(\vec{p})\Big] - n_F\Big[\epsilon(p_x+k, p_y+q)\Big]}{\epsilon(\vec{p}) - \epsilon(p_x+k, p_y+q) + i0^+}, \tag{4.7}$$

coming from the convolution of the two momentum-space Green's functions in Eq. (4.3), where $\epsilon(\vec{p}) = -2(\cos p_x + \cos p_y) - \mu_{2D}$ is the dispersion of the 2D gas and $n_F$ is the Fermi-Dirac distribution. Furthermore, the extra kernel in the mediated interactions is defined as $\Gamma_{ijkl}(q) = \sum_{a,b} e^{iq(b-a)} T_{ai}^* T_{aj} T_{bk}^* T_{bl}$, summing over the leg indices $a, b = 1, 2, \cdots, N$. It is worthwhile to notice that the mediated interactions are the Ruderman-Kittel-Kasuya-Yoshida (RKKY) type [4]. However, the exact profile in real space can not be computed analytically since we consider a lattice model.

## 4.4 Results of the Renormalization

In the absence of the mediated interaction, all bare values of the couplings in RG equations would be the same since only on-site interactions are considered. In the presence of the mediated interactions, this symmetry is broken and the initial couplings renormalize in very different ways, as shown as Eq. (4.5). However, since the mediated interactions are determined only by the exchanged momenta in spin-conserving scattering processes, couplings sharing the same exchanged momenta remain the same bare values. For instance, zero momenta is exchanged in both $c_{ii}^s$ and $f_{ij}^s$ and they therefore have the same bare value, similarly, for $c_{ij}^l$ and $f_{ij}^l$ with exchanged momenta $(k_{F_i} + k_{F_j})$.

The RG equations of a $N$-leg ladder can be found in the literature [57], and

are only solved numerically. After taking the effective interactions as the initial condition and integrating the differential RG equations, the flows of the couplings can be obtained. By analyzing these flows with the scaling Ansatz, $g_i \sim 1/(l_d - l)^{\gamma_i}$, where $l_d$ is the divergent length scale in one-loop RG, the hierarchy of the relevant couplings can be directly read out from the RG exponent $\gamma_i$ [59, 13]. Combining with the Abelian bosonization method, the phase diagram of a ladder system is determined[39, 10, 11].

Furthermore, the relative values of the charge and spin gaps between different Fermi points can be determined by the RG exponents[59]. This allows us to distinguish the $d$-wave superconductivity with an anisotopic spin-gap (referred as $d$-SC$_2$ here) in a two-leg ladder with heavy doping, $n < 0.6$. We note that there is not a real phase transition between the $d$-wave superconductivity with isotropic spin gaps ($d$-SC) and $d$-SC$_2$, because the number of spin and charge gaps and relative sign of relevant couplings are the same. However, it is useful to emphasize this difference here because the anisotropic spin gaps can measured, and therefore the two phases can be distinguished experimentally.

To illustrate how the mediated interaction depends on the filling of the 2D fermions, we show results for $\mu_{2D} = 0$, when the 2D Fermi surface is nested (Fig. 4.2a), and for $\mu_{2D} = 1$ (Fig. 4.2c)[1].

The corresponding phase diagrams are shown in Fig. 4.2b and Fig. 4.2d. In Fig. 4.2b, when the strength of the coupling $U_{cl}/U_l$ is larger than 1.2, a CDW starts to emerge from $d$-SC near half-filling ($n \simeq 1$). Increasing $U_{cl}/U_l$ brings the phase boundary to higher hole-doping. It is interesting to note that the Luttinger liquid phase that appears near $n \gtrsim 0.5$ for the standard Hubbard model [39] is destroyed by the mediated interactions. We find a three-phase "triple-point" (CDW, $d$-SC and $s$-SC)

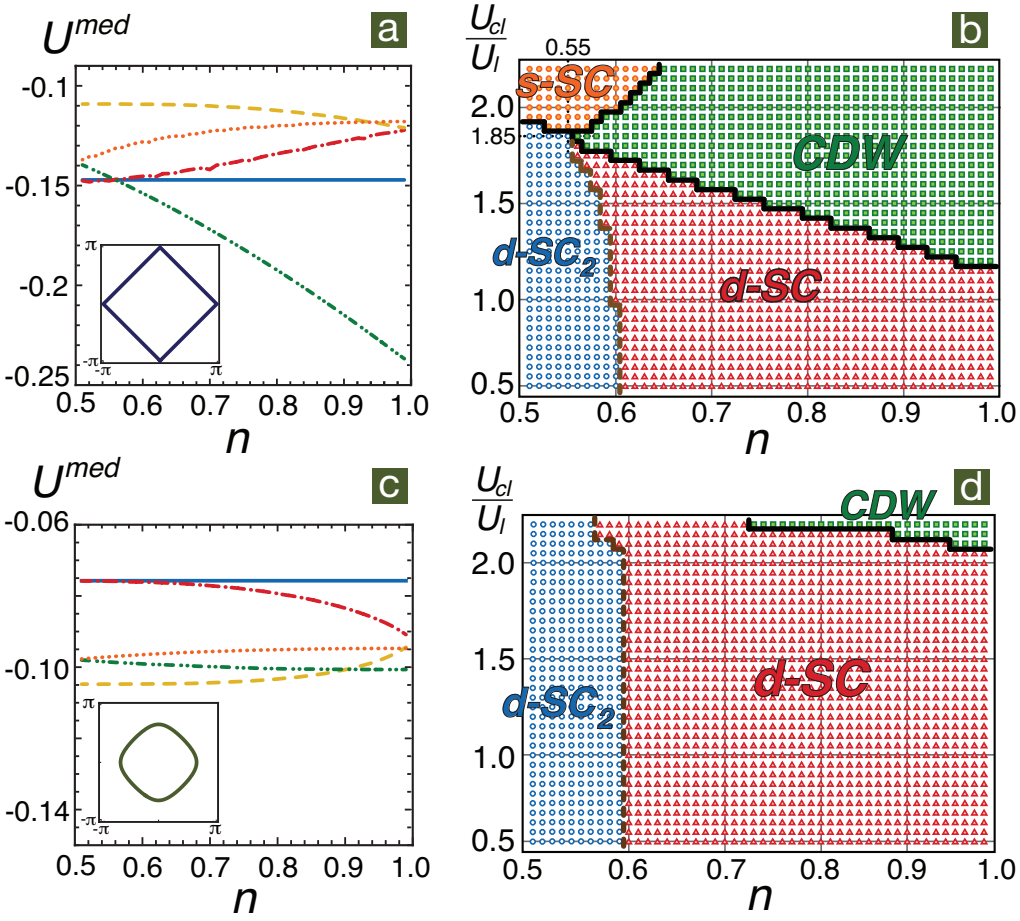


Figure 4.2: Interactions mediated by a 2D gas with (a) $\mu_{2D} = 0$ and (c) $\mu_{2D} = 1$ versus density $n$ of the ladder: The blue solid line represents $c^s_{11}$, $c^s_{22}$ and $f^s_{12}$. $c^l_{12}$ and $f^l_{12}$ are denoted as the green dot-dash-dotted line. The red dot-dashed, orange dotted, and brown dashed lines denote $c^l_{11}$, $c^s_{12}$ and $c^l_{22}$ respectively. The corresponding phase diagrams for (a) and (c) are illustrated in (b) and (d), respectively.

at $U_{cl}/U_l = 1.85$ and $n = 0.55$. From there, increasing the $U_{cl}/U_l$ ratio gives $c^l_{11}(0)$ (or $c^\sigma_{11}(0)$) negative, and an $s$-SC phase occurs, as expected by BCS theory. Doping away from the "triple-point", $f^\sigma_{12}(0)$ becomes negative and CDW dominates. Roughly speaking, when $U_{cl}/U_l > 1.85$, the phase will be determined by the competition between the negative values of $f^\sigma_{12}(0)$ and $c^\sigma_{11}(0)$. It is worthy to notice that though the interaction $U_{cl}$ and $U_l$ are in the limit of weak couplings, the ratio $U_{cl}/U_l$ can be very large.

The arising of the CDW phase emerges is caused by enhanced mediated interactions $f^l_{12}$ near half-filling. When $n \simeq 1$, the momentum exchanged during $f^l_{12}$ processes approaches $\pi$. The particle-hole propagator in the mediated interaction shows a maximum contribution at $\mu_{2D} = 0$, resulting from maximum electron-hole pairing [from $\cos p_x$ and $\cos(p_x + \pi) = -\cos p_x$] in the 2D dispersion along the $x$-direction. Moving away from $n = 1$, the mediated interaction of $f^l_{12}$ decreases, at which point the CDW phase ceases to occur. When we increase the 2D chemical potential, the same behavior occurs. As shown in Fig. 4.2 (d), the regime of the CDW phase shrinks at $\mu_{2D} = 1$ resulting from weak mediated interactions. In this situation the mediated interactions vary smoothly, and show little effect in the ladder system. Therefore, the mediated interaction depends strongly on the chemical potential in the 2D system, and consequently, the phase diagram of a two-leg ladder can be modified/tuned via the filling in the 2D square lattice.

To further illustrate the influence of the 2D density, we show the mediated interactions and corresponding phase diagrams parameterized by the chemical potential in the 2D system in Fig. 4.3 (a)(b) and (c)(d) for fixed density in the ladder, $n = 0.55$ and $n = 0.95$, respectively. When $U_{cl}/U_l$ is larger than 1.2 at $n = 0.95$, the phase transition between CDW and $d$-SC happens near $\mu_{2D} = 0$. However, the phase boundary moves

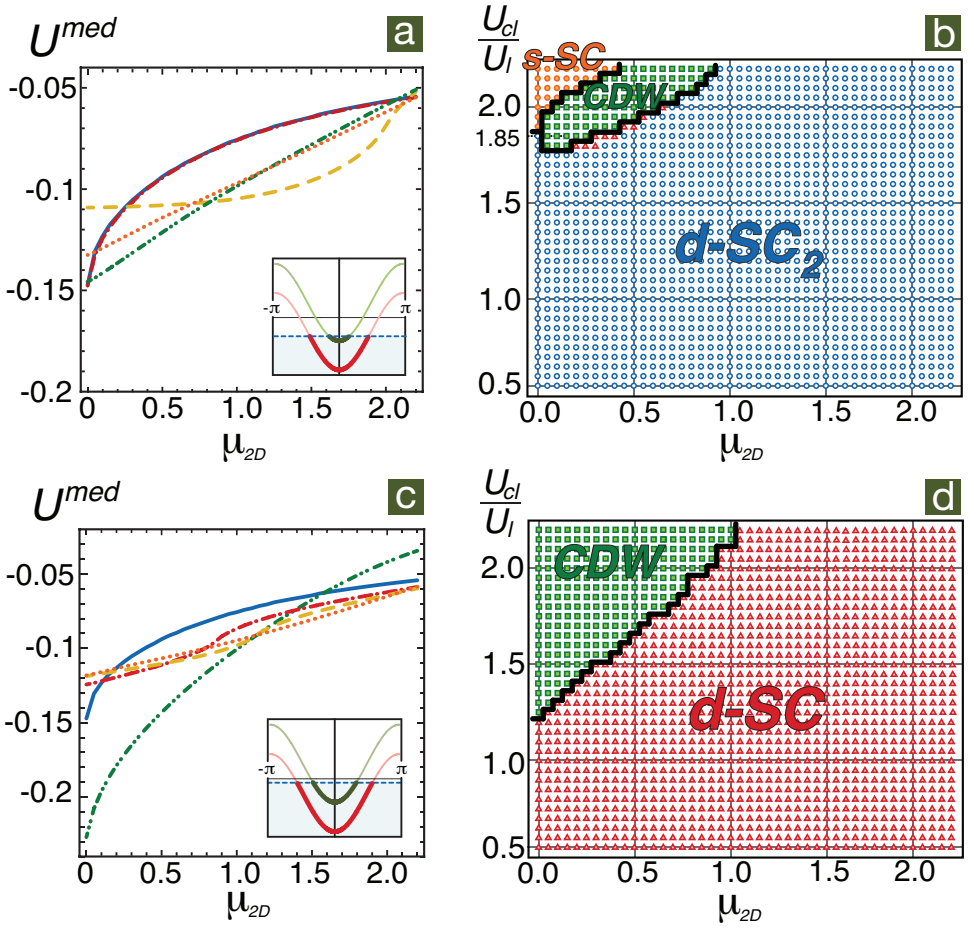


Figure 4.3: The mediated interactions from a 2D gas with densities $n = 0.55$ and $n = 0.95$ on the ladder are plotted as function of the chemical potential $\mu_{2D}$ of the 2D system (in units of the 2D hopping amplitude $t_c$) in (a) and (c), respectively. The strokes for couplings in (a) and (c) are the same as in Fig. 4.2. Corresponding phase diagrams are shown in (b) and (d).

to higher values of $U_{cl}/U_l$ when the chemical potential $\mu_{2D}$ increases and the mediated interaction decreases. In general, the tendency of the mediated interaction is to decrease upon the increasing of the filling in the 2D system (or $\mu_{2D}$), due to the non-interacting assumption. Under this condition, the strength of the mediated interactions is roughly proportional to the density near the Fermi surface, which is maximum at $\mu_{2D} = 0$.

Although the pattern of the mediated interactions in real space is rather complicated, it can be approximated as an effective on-site attraction and a nearest-neighbor repulsion, since longer range terms are rapidly decaying. The phase diagram can then be understood from these two effective interactions. By tuning the chemical potential in 2D, CDW emerges when the effective nearest-neighbor repulsion exceeds the original on-site repulsive interaction. However, increasing the $U_{cl}/U_l$ ratio makes the magnitude of the effective on-site attraction larger than the original on-site repulsion. When the average on-site attraction is weak, CDW and $s$-SC phases compete. Nevertheless, the $s$-SC phase is dominant for large $U_{cl}/U_l$, and the inter-species interaction can be regarded as a glue to pair the fermions, similar to the electron-phonon interaction in a conventional superconductor.

# Chapter 5

# Conclusion

Chapter 3 was concerned with the quantum many-body phases of a 1D/2D mixed dimensional fermionic cold atom system. This sytem is composed of a 1D line embedded into a 2D square lattice where the two species were taken to interact via a density-density interaction on the 1D line. An effective theory for the 1D system was found by first carrying out a partial trace of the partition function with respect to the 2D fermions. This process manifested itself via an effective interaction amongst 1D atoms mediated by 2D atoms. The density of the 2D system influenced the form of this mediated interaction whose values at $k_4 - k_1 = 0, \pi$ directly influenced the quantum many-body phase of the 1D system. The phase diagram could thus be written in the parameter space of $|U_{eff}(0)|$ and $|U_{eff}(\pi)|$. The phase diagram was quite rich indicating instabilities in CDW, SDW, SS, and ST channels, as well as producing regions where the system flowed to a non-interacting fermi liquid and a system described by the Tomonaga-Luttinger model (a.k.a. a Luttinger liquid). In one region however, none of the couplings diverged while back scattering and Umpklapp scattering scaled to zero. This left a model that could be bosonized and the phase was determined by the slowest

decaying correlation function.

Chapter 4 extended the idea of chapter 3 to the two-leg ladder. This system is described by a two-leg ladder embedded into a 2D square lattice. Again, integrating out the 2D system is akin to a mediated interaction between ladder-fermions mediated by the 2D lattice. The presence of the mediated interaction skews the results had the 2D lattice not been present. This is due to the addition of particle-particle and forward scatterings which affect the way the couplings would otherwise renormalize. In this modified system, a d-wave superconducting state with an anisotropic spin-gap develops with heavy doping, $n < 0.6$ Increasing the density sees the emergence of CDW, d-SC and s-SC phases. One novel attribute of the system is the quenching of the typical Luttinger liquid phase due to the presence of the mediated interaction. Although precise analytical forms for the mediated interaction in real space are complicated, there seems to be an overall pattern of on-site attraction and nearest neighbor repulsion. By looking at the phase diagram as parameterized by the 2D chemical potential, one gets a better feel for the way the 2D chemical potential acts as a knob, directly tuning the phase for the ladder system.

Thus we have shown how systems that have been studied in depth in the past have seen new growth in the application of connecting them to systems of higher dimensions. The presence of the higher dimensional system (in this case 2D) manifests itself as an effective interaction amongst the lower dimensional fermions. In both cases, the chemical potential of the 2D system acts as a knob with which the phases of the 1D/ladder system may be tuned.

# Bibliography


[1] It is important to mention that if the self-energy correction from integrating the 2D system is included, a fixed chemical potential in the 2D system means varied fillings according to $U_{cl}$ and the filling of the two-leg ladder.

[2] M. Abramowitz and I. A. Stegun. *Handbook of Mathematical Function with Formulas, Graphs, and Mathematical Tables*. Dover, New York, 1972.

[3] A. A. Abrikosov, L. P. Gorkov, and I. E. Dzyaloshinski. *Methods of Quantum Field Theory in Statistical Physics*. Dover Publications, New York, 1975.

[4] Neil W. Ashcroft and N. David Mermin. *Solid State Physics*. Thomson Learning, 1976.

[5] A. Atland and B. Simons. *Condensed Matter Field Theory*. Cambridge University Press, Cambridge, 2006.

[6] L. Balents and M. P. A. Fisher. *Phys. Rev. B*, 53:12133, 1996.

[7] I. Bloch. *Nature Phys.*, 1:23, 2005.

[8] I. Block, J. Dalibard, and W. Zwerger. *Rev. Mod. Phys*, 80:885, 2008.

[9] C. Bourbonnais and L Caron. *Int. J. Mod. Phys. B*, 5, No. 6:1033–1096, 1991.

[10] J. E. Bundler and H.-H. Lin. *Phys. Rev. B*, 78:035401, 2008.

[11] J. E. Bundler and H.-H Lin. *Phys. Rev. B*, 79:045132, 2009.

[12] A. C. Voigt et al. *Phys. Rev. Lett.*, 102:020405, 2009.

[13] Y. Cai, W.-M. Huang, and H.-H. Lin. *Phys. Rev. B.*, 85:134502, 2012.

[14] Herbert B. Callen. *Thermodynamics and an Introduction to Thermostatistics*. John Wiley and Sons, 1985.

[15] M.-H. Chang, W. Chen, and H.-H. Lin. *Prog. Theor. Phys. Suppl.*, 160:79, 1995.

[16] C. Chin, R. Grimm, P. Julienne, and E. Tiesinga. *Rev. Mod. Phys.*, 82:1225, 2010.

[17] F. Dalfovo, S. Giorgini, L. Pitaevskii, and S. Stringari. *Rev. Mod. Phys.*, 71:463, 1999.

[18] V. J. Emery. *Highly Conducting One-Dimensional Solids*. Plenum, New York, 1979.

[19] Alexander L. Fetter and John Dirk Walecka. *Quantum Theory of Many-Particle Systems*. Dover, New York, 2003.

[20] S. G. Bhongale, L. Mathey, S. W. Tsai, C. W. Clark, and E. Zhao. *Unconventional Spin Density Waves in Dipolar Fermi Gases*.

[21] S. G. Bhongale, L. Mathey, S. W. Tsai, C. W. Clark, and E. Zhao. *Phys. Rev. Lett.*, 108:145301, 2012.

[22] T. G. Tiecke et al. *Phys. Rev. Lett.*, 104:053202, 2010.

[23] C. H. Wu et al. *Ultracold Fermionic Feshbach Molecules of* $^{23}Na^{40}K$.

[24] F. D. Haldane. *J. Phys.*, C14:2585–2919, 1981.

[25] E. Haller et al. *Phys. Rev. Lett.*, 104:153203, 2010.

[26] J. Hubbard. *Proc. R. Soc. London*, 276:238–257, 1963.

[27] M. Iskin and A. L. Subasi. *Phys. Rev. A*, 82:063628, 2010.

[28] D. Jaksch, C. Bruder, J. Cirac, C. Gardiner, and P. Zoller. *Phys. Rev. Lett.*, 81:3108, 1998.

[29] D. Jaksch and P. Zoller. *Ann. of Phys*, 315:52, 2005.

[30] K. K. Ni et al. *Science*, 322:231, 2008.

[31] L. P. Kadanoff, W. Götze, D. Hamblen, R. Hecht, E. A. S. Lewis, V. V. Palciauskas, M. Rayl, and J. Swift. *Rev. Mod. Phys.*, 39, No. 2:395, 1967.

[32] J. F. Kenney and E. S. Keeping. *Mathematics of Statistics*, volume 2. Van Nostrand, Princeton, NJ, 1951.

[33] W. Ketterle and N. J. van Druten. *Adv. At. Mol. Opt. Phys.*, 96:181, 1997.

[34] F. D. Klironomos and S.-W. Tsai. *Phys. Rev. B*, 74:205109, 2006.

[35] Alok Kumar. *arXiv*, 1002.4692, 2010.

[36] C. Lai, C. Shi, and S. W. Tsai. *Phases of Population Imbalanced Fermi-Fermi Mixtures on an Optical Lattice*.

[37] G. Lamporesi et al. *Phys. Rev. Lett.*, 104:153202, 2010.

[38] A. Legget. *Rev. Mod. Phys.*, 73:307, 2001.

[39] H.-H. Lin, L. Balents, and M. P. A. Fisher.

[40] H.-H. Lin, L. Balents, and M. P. A. Fisher.

[41] M. Lu, N. Q. Burdick, and B. L. Lev. *Phys. Rev. Lett.*, 108:215301, 2012.

[42] J. M. Luttinger. *J. Math. Phys.*, 4:1154–1162, 1963.

[43] F. M. Marchetti, Th. Jolicoeur, and M. M. Parish. *Phys. Rev. Lett.*, 103:105304, 2009.

[44] F. M. Spiegelhalder et al. *Phys. Rev. Lett.*, 103:223203, 2009.

[45] E. Miranda. *Brazilian Journal of Physics*, 33, 1:3, 2003.

[46] John Negele and Henri Orland. *Quantum Many-Particle Systems*. Westview Press, 1998.

[47] Y. Nishida. *Phys. Rev. A*, 82:011605, 2010.

[48] Y. Nishida and S. Tan. *Phys. Rev. Lett.*, 101:170401, 2008.

[49] Y. Nishida and S. Tan. *Phys. Rev. A*, 79:060701, 2009.

[50] Y. Nishida and S. Tan. *Phys. Rev. A*, 82:062713, 2010.

[51] G. Partridge, W. Li, R. Kamar, Y. Liao, and R. Hulet. *Science*, 311:503, 2006.

[52] G. Partridge et al. *Phys. Rev. Lett.*, 97:190407, 2006.

[53] C. Pethick and H. Smith. *Bose-Einstein Condensation in Dilute Gases*. Cambridge Universty Press, Cambridge, 2001.

[54] L. Pitaevskii and S. Stringari. *Bose-Einstein Condensation*. Oxford University Press, Oxford, 2003.

[55] L. Pollet, M. Troyer, K. V. Houcke, and S. M. A. Rombouts.

[56] Antoine Royer. *J. Math. Phys.*, 25:2873, 1984.

[57] A. Seidel, H.-H. Lin, and D.-H. Lee. *Phys. Rev. B*, 71:220501, 2005.

[58] R. Shankar. *Rev. Mod. Phys.*, 66:129, 1994.

[59] H.-Y. Shih, W.-M. Huang, S.-B. Hsu, and H.-H. Lin. *Phys. Rev. B.*, 81:121107, 2010.

[60] Y. Shin. *Phys. Rev. Lett.*, 97:030401, 2006.

[61] Y. Shin et al. *Nature*, 451:689, 2008.

[62] M. Taglieber et al. *Phys. Rev. Lett.*, 100:010401, 2008.

[63] S. Taie et al. *Phys. Rev. Lett.*, 105:190401, 2010.

[64] E. Timmermans, P. Tommasini, M. Hussein, and A. Kerman. *Phys. Rep.*, 315:199, 2009.

[65] S. Tomonaga. *Prog. Theor. Phys.*, 5:544–569, 1950.

[66] A. Trenkwalder et al. *Phys. Rev. Lett.*, 106:115304, 2011.

[67] D. J. Wallace and R. K. P. Zia. *Ann. Phys.*, 92:142, 1975.

[68] G. H. Wannier. *Phys. Rev.*, 52:191, 1937.

[69] G. H. Wannier. *Rev. Mod. Phys.*, 34:645, 1962.

[70] E. Willie et al. *Phys. Rev. Lett.*, 100:053201, 2008.

[71] K. G. Wilson. *Phys. Rev. B*, 4, No. 9:3174–3183, 1971.

[72] D. Zanchi and H. J. Schulz. *Phys. Rev. B*, 61, 20:13609, 2000.

[73] W. Zwierlein. *Nature (London)*, 442:54, 2006.

[74] W. Zwierlein, A. Schirotzek, C. H. Schunck, and W. Ketterle. *Science*, 311:492, 2006.